Ecological Indicators 158 (2024) 111583

Contents lists available at ScienceDirect

Ecological Indicators

journal homepage: www.elsevier.com/locate/ecolind

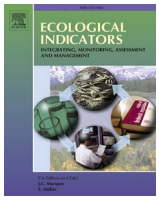

Original Articles

Combining biodiversity and geodiversity on landscape scale: A novel approach using rare earth elements and spatial distribution models in an agricultural Mediterranean landscape

Samuel Pelacani [a,*], Michael Maerker [b,c,d], Simone Tommasini [a], Sandro Moretti [a]

[a] Earth Sciences Department, University of Florence, Italy
[b] Leibniz Centre for Agricultural Landscape Research, Müncheberg, Germany
[c] Department of Earth and Environmental Sciences, University of Pavia, Via A. Ferrata 1, 27100 Pavia, Italy
[d] Centro Nazionale delle Ricerche, Istituto di Geoscienze e Georisorse IGG, Via A. Ferrata 1, Pavia, Italy

ARTICLE INFO

Keywords:
Rare Earth Elements
Geomorphometry
Biodiversity
Geographic food authentication
Olive orchard
Tuscany Region

ABSTRACT

Landform diversity influences and interacts with both biodiversity and geodiversity and thus, they are key factors in the assessment of landscape resilience. However, research on the spatial relationships between landscape geodiversity and biodiversity is challenging because we are still lacking methods to link abiotic with biotic factors. The goal of this study is to explore and quantitatively assess the spatial relationship between geomorphometric factors and the relative distribution of rare earth elements (REEs) in soils and organism. Therefore, we selected a representative Mediterranean landscape characterized by ancient olive grove cultivations. The results show for different landforms and lithotypes a positive linear correlation in the lanthanum/samarium *vs.* lanthanum/ytterbium (La/Sm *vs.* La/Yb) signature between the bioavailable fraction of topsoil and olive drupe. Results of La/Yb *vs.* La/Sm reported as power function for olive drupes and topsoil follow comparable scaling ranges showing a power law of 0.83 and 0.71 respectively with an R^2 0.96 *vs.* 0.71. A different scaling range behavior from topsoil to the related olive drupe was found for each parent rock material. Results of the Machine Learning (ML) modelling framework showed that the La_N/Sm_N in topsoil, were substantiality correlated to channel network base level, topographic wetness index, NDWI and valley depth. Under the physiographic environmental variables of the study area, the spatial distribution of La_N/Yb_N was mainly related to the lithological characteristics. Furthermore, NDVI was the most important variable to predict the fractionation ratio of La_N/Yb_N in olive drupe and the topographic channel network distance for La_N/Sm_N in olive drupe. Our findings provide new insights in the spatial distribution of REEs allowing an assessment of bio- and geodiversity of olive groves taking into account biophysical factors. Our research represents a starting point for future applications and modelling techniques to analyze at the catchment-scale the REEs biophysical fluxes and food traceability.

1. Introduction

Geodiversity incorporates both static and dynamic physical components of the environment, ranging from topography, rocks, soils and landforms, to geomorphological, hydrological and soil processes (Gray, 2021; Serrano and Ruiz-Flano, 2007). The interactions of geodiversity and climate variables are important for sustaining biodiversity and the ecosystem services they provide through water availability and inorganic elements (Hjort and Luoto, 2010).

It is well known how topographical variations can influence the macro-/ micro-climate of an area (Alexander et al., 2016), soil composition and dynamics (Milne, 1936; Jenny, 1941; Ruhe and Walker, 1968; Montgomery et al., 2000) and shape the structure and function of a landscape (Jucker et al., 2018; Perez Sanchez et al., 2023; Dauphin et al., 2023). Geodiversity is considered the basis of heterogeneity of the landscape (Parks and Mulligan, 2010; Bailey et al., 2017). In fact, the

Abbreviations: CNBL, Channel Network Base Level; VD, Valley Depth; CND, Vertical Distance to Channel Network; TRI, Terrain Ruggedness Index; TPI, Topographic Index; TWI, Topographic Wetness Index; NDVI, Normalized Difference Vegetation Index; NDWI, Normalized Difference Water Index; GEO, Lithology; La_N/Sm_N and La_N/Yb_N, respectively, lanthanum/samarium and lanthanum/ytterbium normalized to Upper Crust Continental.

* Corresponding author.
E-mail address: samuel.pelacani@unifi.it (S. Pelacani).

https://doi.org/10.1016/j.ecolind.2024.111583
Received 6 August 2023; Received in revised form 5 January 2024; Accepted 11 January 2024
Available online 20 January 2024

areas with high geodiversity provide a wide range of environmental mosaics and corridors that allow different species and communities to persist, adapt or move where there is adequate connectivity both, within and between different landforms and geomorphological systems (Brierley et al., 2006; De Falco et al., 2021). Indeed, geomorphological processes help to maintain or increase the heterogeneity of the landscape and habitat, a key factor to improve landscape resilience (Stein et al., 2014; Pettersson and Jacobi, 2021). This concept has been particularly addressed by the Conserving Nature's Stage (CNS) approach, which focusses on the use of geodiversity in conservation planning (Hunter et al., 1988; Anderson and Ferree, 2010).

Although many authors have stressed the importance of quantifying geodiversity using objective evaluation procedures that can be repeated and correlated to indices used in biodiversity and pedodiversity studies, up till now research studies that have explored the spatial variability of both geodiversity and biodiversity are still largely lacking (Hjort and Luoto, 2010; Syrbe and Walz, 2012; Zarnetske,et al., 2019; Ibáñez et al., 2021; Ibáñez and Brevik, 2022; Laush et al., 2020; Tukiainen et al., 2022).

In order to fill this gap, the present study represents a first step towards a deeper insight concerning the spatial characteristics of REEs in abiotic and biotic systems. Therefore, we propose an innovative approach that combines REEs and spatial distribution models in an agricultural Mediterranean landscape. Moreover, this study explores the possibility to develop new indicators to monitor food origin and the impacts of the REEs on the environment and the related organisms. This is important for assessing the food safety, especially in Mediterranean countries where extra virgin olive oil is generally consumed in high quantities and on daily basis. We conduct a scenario analysis on the spatial distribution of REEs at basin scale, focusing on an organic olive agricultural production system and conservative practices (Kavvadias and Koubouris, 2019).

Using trace element signatures, we directly assess the processes linking soil geochemical anomaly to plant uptake without using a surrogate index (see also Rate and Ma, 2010) and thus, the direct connection between abiotic and biotic factors. The term of *geochemical anomaly* refers to an enrichment (positive anomaly) or depletion (negative anomaly) of an individual REE in relation to a background value. Specifically, to a value detected in olive drupe with respect to its soil of origin. A landscape connectivity approach helps us to understand how and whether the biogeochemical fluxes of less mobile trace elements are controlled by soil erosion/deposition processes, soil solute transport and vegetation uptake.

To this end, the present research, targets at the landscape scale focusing on the integration of landform, geochemistry and biodiversity in agricultural-dominated landscapes, to establish relationships between the specific elements. Machine learning (ML) techniques were applied to detect the geometric signatures (Pike, 1988; Giles, 1998; Iwahashi and Pike, 2007) of structural landforms, that influenced the soil development in secular olive groves, to assess quantitatively the current regional bio-geodiversity among the main geological settings of Tuscany.

In general, landform types are conditioned by the lithologies but on the other hand landforms influenced the development of a given type of land use (Liao et al., 2019). In fact, the environmental factor exerts a strong influence on the development of a certain agricultural system, such as the construction of graded terraces to cultivate on steep slopes, e.g. arenaceous or marly-arenauceous slopes of the Chianti area (Tuscany, Italy; Fig. 5). Hence, in the present research we focus on landform types taking into account the connection between lithology and the development of a given land management.

From a "geographic traceability" point of view, it is important to quantify the spatial–temporal patterns of REEs in topsoil and plant fruits (olive drupe) to explore the linkage between landforms of different origins and ages.

REE cycles in the biosphere are still poorly understood, with conflicting evidence and opinions on biological effects, their cycles and their role in biological systems (Chen et al., 2001; Tyler, 2004; Kovaříková et al., 2019). Correlations between REE species in natural soil system and their bioavailability are still unclear (Kovaříková et al., 2019) due to the fact that only a few studies have considered natural growing conditions (Brioschi et al., 2013; Censi et al., 2014; Pošćić et al., 2020). Moreover, these studies often lack information about the control and quality checks of the analyses and hence, does not allow to evaluate the validity of the results or to make comparisons between the different studies.

A recent investigation showed how REEs are transported via xylem sap in *Vitis vinifera* L. and that there is no clear selection of REEs, rather their content is related to the bioavailability of the substrate REEs (Barbera et al., 2023). Another previous study found that the REE translocation from soil to olive drupe is soil dependent (Pošćić et al., 2020). Studies on *Vitis vinifera* L. reported that elements from samarium to holmium are concentrated in root tissue, europium in the aerial part and from lanthanum to samarium in berries (Bertoldi et al., 2009; Censi et al., 2014).

REEs, also called lanthanides, include the 15 elements (atomic number 57–71), and according to their physical and chemical properties, REEs are usually divided into Light Rare Earth Elements (LREEs from La to Sm), Medium Rare Earth Elements (MREEs from Sm to Gd) and Heavy Rare Earth Elements (HREEs from Gd to Lu). LREEs are more abundant than HREEs in rocks and soils (Tyler, 2004), and, as a whole, are highly electropositive and predominantly trivalent, with the exception of cerium in some specific environments such as under oxidizing conditions ($Ce3+ \rightarrow Ce4+$) and europium under reducing conditions ($Eu3+ \rightarrow Eu2+$) (Brookins, 1989). The natural occurrence of the REEs depends on different geological characteristics and has been subject of interest for geologist as a tool for tracing natural geochemical evolution processes of various systems (Henderson, 1984; Brioschi et al., 2013; Catrouillet et al., 2019). The key role of REEs in the identification of sedimentary sources is based on the assumption that they are relatively conservative (Wang et al., 2019). REEs reflect the mineralogical and geochemical signatures of the rocks and indicate the geochemical evolutionary processes of the sedimentary systems (Aide and Aide, 2012; Khan et al., 2017). Pelacani et al. (2017) found a distribution of REEs in olive drupe showing the same patterns of their respective soils with the exception for cerium and europium. Indeed, olive drupe from different soils show variable REEs patterns allowing to trace their origin (Pelacani et al., 2017; Barbera et al., 2022).

The REEs dataset used in our investigation comprise 14 elements of REEs from lanthanum to lutetium and accounts for a wide variation of geological environments, providing information linking different soil-forming factors to pedogenic processes, allowing for a better understanding on the impacts of human activities and natural variations on soil REEs geochemistry. Our hypothesis is that the variability of soil-REE concentrations and olive drupe REEs fractionation is strongly influenced by parent material, topographic features, soil erosion and hydrological processes, as well as land use and biomes (Zaharescu et al., 2017).

Within the framework of the EIP-AGRI European Project on rural development 2014–2020 for Operational Groups, we started from a case study in Tuscany to improve our understanding how biodiversity relates to different drivers of geodiversity at different spatial scales to support conservation decisions. Hence, in this study we aim to answer three interrelated questions: (1) Which environmental factors are the main predictors related to the specific lithotypes? (2) What are the individual effects of the environmental key predictors on topsoil REEs distribution? (3) Are the key predictors also related to olive drupe REEs distribution?

To answer these questions, we analyzed an extensive empirical dataset extracted from a Digital Terrain Model (DTM) and additional remotely sensed data (Sentinel-2) covering a wide range of geographic settings. To assess the spatial distribution and relationships between REEs and the bio- and geo-diversity we utilized a combined geostatistical approach based on stochastic gradient boosting regression tree (SGB) and multivariate adaptive regression splines (MARS).

2. Materials and methods

2.1. Geological setting of the study area

In this study we focused on the Greve stream watershed with a drainage area of 272 km^2, a left tributary of the Arno river, located in the Chianti area about 10 km south to southwest of Florence, Tuscany, Italy. The altitude ranges between 71 m and 913 m a.s.l. (Fig. 1).

In the watershed there are three non-metamorphic tectono-sedimentary units outcropping reported in the Supplementary Material (see Appendix A1). The most widely distributed tectonic element that is characterized by ancient olive grove cultivations are the allochthonous sediments belonging to the External Ligurian Domain (Mt. Morello units; Bortolotti, 1964): Morello Formation, Sillano Fm. (Principi and DeLuca-Cardillo, 1975) and Pietraforte Formation, followed by the Tuscan Nappe. The Macigno Formation, is a tectonic unit belonging to the Tuscan Domain. Moreover, we find post-orogenic fluvial deposits outcropping on the western flanks of the basin (Plio-Pleistocenic deposits, VILa). The Ligurian Mt. Morello units are exposed in the westernmost sector of the study area and they are represented by deep-seated turbidite successions. The latter are characterized from bottom to top by: fine turbidite dark-gray limestones, dark-brownish and polychromous shales (Sillano Fm. - SILL, late Cretaceous – early Eocene) with interbedded coarse lens-shaped bodies of hybrid/mixed turbidite fine grained quartz-calcareous siltstones ('Pietraforte'Fm. - PTF); white-yellowish fine limestones, marly limestones and sporadically clayey marls and calcarenites (Mt.Morello Fm. - MLL, early-middle Eocene). The inner portion of the Ligurian domain is characterize by deformed dark shales and silica-rich limestones, quartz-rich siltstones/sandstones, marls and light gray to hazelnut calcareous turbidites ('Palombini'

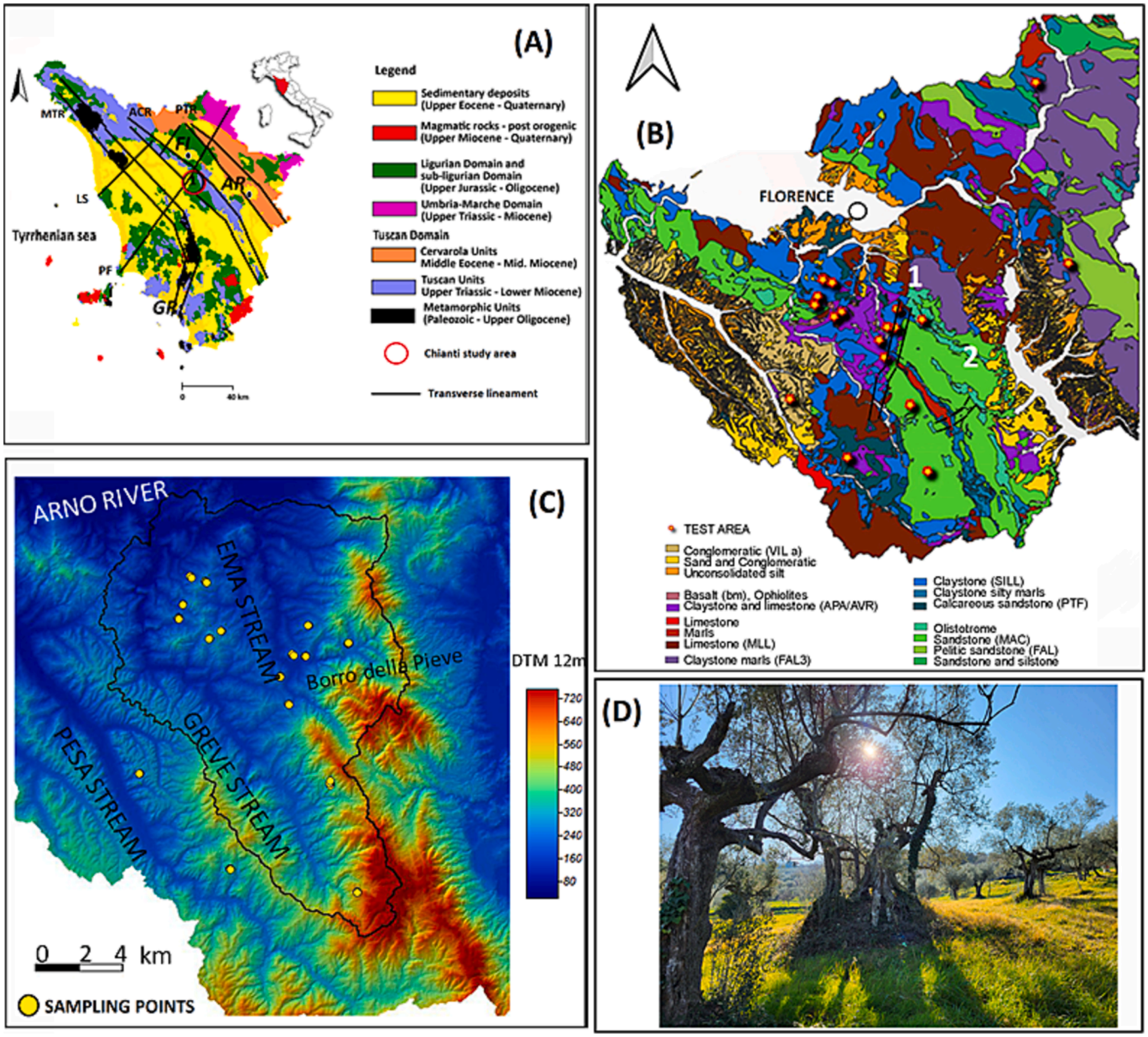

Fig. 1. **(A)** Tectonic sketch of Tuscany with morpho-structural ridges and transverse lineament: "MTR" Middle Tuscan Ridge; "ACR" Abetone-Cetona Ridge; "PTR" Pratomagno-Trasimeno Ridge; "PF" Piombino-Faenza line and "LS" Livorno-Sillaro line. Main cities: FI – Florence, AR – Arezzo, GR – Grosseto. **(B)** Lithologic map of the Chianti Mts, with structural boundaries: (1) Greve-Sezzate fault and (2) Dudda-Incisa fault. **(C)** Digital elevation model of the Greve basin and the location of soil and olive drupe site sampling. **(D)** Ancient olive tree of cultivar moraiolo located in Chianti area. From the soil erosion, about 1.10 m depth, taking into account a medium erosion rate of 1.9 mm yr^{-1} (Montgomery, 2007; Thaler et al. 2012) it could be estimated the olive tree to be around 600 years old.

Shales Fm. - APA; early Cretaceous) with interbedded fragments of ophiolitic complexes (basalts - bm, gabbros, serpentinite breccias and reddish cherts). The Sillano Formation is a chaotic body (Festa et al., 2010) of mixed rocks of different ages and origin such as the varicolored shales (AVR, green, gray, brown, red) alternating quartz-rich or carbonaceous turbiditic sandstones and siltstones, marls and calcareous marlstones.

The 'Macigno' Sandstones, exposed in the eastern sector of the study area ('Macigno' Fm. - MAC; Chattian-Aquitanian), is the uppermost unit of the Tuscan Nappe with a thickness of up to 1,500–2,000 m (Merla, 1969) of siliciclastic turbidite sandstones and siltstones. Furthermore, the 'Macigno' Fm. hosts interbedding with up to 50 m thick lenticular successions of gray-yellowish hemipelagic marls and very fine/distal turbidites (San Polo Marls – "Marne").

2.2. Drainage network and geomorphology

The actual drainage network of the Greve watershed is characterized by mostly NW-NE oriented streams that drain into the Arno River. The Greve watershed is bordered to the SW by the Middle Tuscan Ridge (MTR) and to the NE and SE by the ridge of the Albano - Chianti Mounts (ACR; Fig. 1**a**). These ridges are formed by tectonic-sedimentary units, Ligurian and Tuscan units, related to different paleogeographic and geodynamic domains, dating back to the early Mesozoic and stacked in thrust bands of the Cenozoic fold resulting from the continental European-African collision (Vai, 2001). Further relevant structural elements are represented by the regional distribution of transversal features of the basin (Fazzini and Gelmini, 1982; Pascucci et al., 2007), such as the Livorno-Sillaro fault line (LS) in the NW and Piombino-Faenza fault line (PF) in the SE (Fig. 1**a**). Hence, the drainage network of the study area has been affected by several tectonic/stratigraphic domains, divided by transversal lineaments and belts that are parallel to the main Northern Apennines transversal tectonic lineaments (Pascucci et al., 2007). A series of WSW-ENE or SSW-NNE tectonic lineaments, representing strike-slip faults, bounds the structural and stratigraphic domains (Fig. 1**b**). The main tectonic lineaments are (Fig. 1**b**): the Greve-Sezzate, the Dudda-Incisa and the Badiaccia-*Ponte agli Stolli* Belt (Cornamusini et al., 2011).

Streams are largely parallel to local structures such as faults (Fig. 1). The Eastern part of the catchment is characterized by a dendritic network with oval shape sub-basins. The Ema stream is characterized by convex gentle slopes especially where the stream drains towards the Ligurid outcrops. The eastern side and upper part of the Ema basin where the drainage network is developed on Tuscan nappe formations is mainly dominated by fluvial and slope processes. The related morpho-sculptural landforms are shaped and incised by approximately SW–NE oriented valleys, resulting in narrow crests.

Compared to the eastern sub-catchments, western ones, the rectangular basin shape of the main Greve torrent is characterized by trellis networks, with initial river flows in NW direction and subsequently in NE direction. This marked change in flow direction, or hairpin turn, is accompanied by a large increase in river gradient and local relief. This rectangular basin is characterized by an asymmetric location of the main drainage within the basin.

On the western flank of the Chianti range, rivers generally flow perpendicular to local structures and cross major range-bounding faults. Furthermore, several points along the range crest are characterized by high-elevation, low-relief surfaces. Nonetheless the main drainage divide (MDD) and topographic crests are largely coincident. There are several regions where the MDD and crests are offset (Fig. 1**c** "*Borro della Pieve*").

2.3. The olive groves of the study area

The olive groves together with the production of grapes represent the main economic crops for this Mediterranean basin with a high landscape value (Santoro et al., 2020). Where *Chianti Classico* Wine and Extra Virgin Olive Oil PDO (Protected Designations of Origins) are produced, as well as Extra Virgin Olive Oil *Toscano* PGI (Protected Geographical Indications). The total area of olive grove amounts to 6,012 ha corresponding to circa 22 % of the total area of the Greve basin. The median areal extension of single olive groves is about 0.9 ha, but the most frequent extent of single groves is equal to 0.175 ha.

In terms of the farming management the most common regime is the traditional rainfed olive grove. The Greve basin shows a high biodiversity in terms of olive cultivars (*Olea europaea*) sometimes dating back six centuries, such as the Moraiolo olive (Fig. 1**d**) that is an indigenous cultivar of Tuscany, which has spread across the boundaries of the region to the rest of central Italy. The organic farming management practices are widespread in the Chianti area and intercropping land use management systems are very common (Fig. 5) such as with "*giaggiolo*" (*Iris germanica*) or legumes (*Vicia faba minor*) and mixed crops with ancient rows of vines (*Vitis vinifera* L.). Furthermore, graded terrace management practices are quite common.

The cultivation of the olive trees is not homogeneously distributed among the different lithologies, but none of those is exempt from the presence of olive groves in turn linked to the morphological conditions and the geochemistry of soils. The olive trees are mainly cultivated on gentle slopes characterized by calcareous soils derived from limestones and polychromous shales as parent material (SILL formation) for about 27 %, followed by marly limestones and calcarenites (MLL) for 21 %, by arenaceous (MAC) for 9 % and to a lesser extent by ophiolites and basalts with less than 1 %.

2.4. Soil and olive fruit sampling design and REE laboratory analyses

Soil samples were collected from 17 olive groves belonging to six different geochemical environments of the study area characterized by the following substrates (Fig. 1): claystone, limestone, siltstone, sandstone, magmatic rocks and paleoenvironment conglomerate siltstone. These environments are characterized by the same macro-climatic conditions, but differ in terms of lithology and hence, soil types. The sampling campaign was repeated for two seasons 2020–2021 and from each olive grove 5 soil samples were collected from topsoil in the first year and 3 soil samples in the second year in the same location, for REEs analysis. The selection of olive groves was conditioned by the opportunity to get the olive drupe produced from the olive grove under monitoring. For this reason two olive groves on PTF and Vila lithology were sampled outside of the Greve basin but in the neighboring Pesa basin (Fig. 1). Moreover, taking into account that the Greve basin is characterized by geomorphodynamically induced landforms, the soils were sampled from olive groves lying in the upper parts of the relief, where the soil horizons mainly develop from the bedrock material avoiding colluvial parts. If these conditions were not satisfied, the soil hillslope catena concept (Ruhe and Walker, 1968) was taken into consideration for soil sampling. In correspondence to the olive tree where the soil was sampled in spring ($N_{soil} = 136$ samples), the olives were sampled in October ($N_{olive} = 136$).

The REEs in soils were analyzed by a quadrupole Inductively Coupled Plasma Mass Spectrometry (ICP-MS; Agilent Technologies 7900 ICPMS – Hachioji, Tokyo, Japan) equipped with technology to remove polyatomic interferences, in collaboration with the laboratory Biochemie Lab. (Florence, Italy), as bioavailable fraction. The reproducibility of measurements was assessed combining an internal standard normalization by rhodium and an external calibration using the AGV-1 certified reference materials (Supplementary Material Tab. S4, S5, S6). The accuracy (RSD) for all of the estimated elements varied from 2 to 12.9 % at the μg g^{-1} levels of concentration. The incertitude of the analytical determinations was <10 % at the ng kg^{-1} levels of concentration. The soils were treated with DTPA at pH 5 (Ehlers and Luthy, 2003; Feng et al., 2005) to simulate the natural capability of the rhizosphere to extract REEs from the soil. Each single sample was

measured three times. The bioavailable fraction was extracted by treating 10 g of dried soil with 20 mL of 5 mM DTPA solution at pH 5. The obtained suspension was stirred for 24 h at 25 °C, filtered with Millipore™ membranes (0.45-μm membrane filter) and diluted 50 times. Furthermore the REEs were analyzed by a quadrupole ICP-MS in olive drupe. The pulp and pit were treated with 4 mL of HNO_3 of ultrapure grade two times, spaced one half-hour, by using also 2.5 mL of ultrapure-grade H_2O_2. After digestion, the extracts were diluted with ultrapure water to 15.0 mL (Barbera et al., 2022).

2.5. Model structure and workflow

The basic idea was to find automatically selected terrain covariates using Machine Learning (ML) approaches to analyses the relationships between geodiversity and biodiversity of the study area (Fig. 1). Following our hypothesis geodiversity and biodiversity can be traced using REEs geochemical composition that in turn is strictly related to landforms defined as a distinctive feature of the land surface shaped by erosion, accumulation or deformational processes.

Using SAGA GIS, we applied a detailed digital terrain analysis to quantify and describe the terrain landforms through topographic indices extrapolated from a 12 × 12 m cell size-resolution DTM (see Märker et al., 2011; Maerker et al., 2020; Adeniyi et al., 2023) obtained from the TanDEM-X radar imaging satellite platform provided by the Deutsches Zentrum für Luft und Raumfahrt (DLR). The DTM was pre-processed in order to extract artefacts and to guarantee hydrological functionality (fill sinks) using the algorithm proposed by Wang and Liu (2006). Subsequently, the following terrain indices have been derived in SAGA GIS from the pre-processed DTM, reported in the Supplementary Material (see Appendix A2): (i) three basic terrain derivatives (slope, aspect and catchment area); (ii) terrain ruggedness index (TRI) following Riley (1999); (iii) topographic wetness index (TWI) based on modified catchment area and slope tangent (Sørensen et al., 2005); (iv) valley depth (VD); (v) channel network base level (CNBL) and (vi) vertical distance to channel network (CND) (Conrad et al., 2015); (vii) Length Slope Factor (LS Factor) following Conrad et al. (2015); Topographic Position Index (TPI) (Guisan et al., 1999) defined as the difference between a central pixel and the mean of its surrounding pixels. Terrain Ruggedness Index (TRI), in contrast, is the mean of the difference between the central pixel and its surrounding pixels (Riley et al., 1999).

The two environmental information layers are represented by the lithotypes (Fig. 1) and land use data (Tuscany Region, 2020). The Normalized Difference Vegetation Index (NDVI; Rouse et al., 1973) and the Normalized Difference Water Index (NDWI; McFeeters, 1996) were derived from remote-sensing data. The NDVI is useful to understand the distribution of vegetation and provides information about the relation between vegetation cover and bare soil. The NDWI is also a remote sensing based indicator sensitive to the change in the soil water content or in the water content of leaves (Gao, 1996). The NDVI and NDWI data were extrapolated from Advanced Spaceborne Thermal Emission and Reflection Radiometer (Sentinel-2) images. One image from 27.06.2020 was downloaded from USGS Earth Explorer, and corresponds to the same period of the soil sampling survey. The NDVI was calculated applying the formula: NDVI = (Band 8-Band 4)/(Band 8 + Band 4) and the NDWI was calculated applying the formula NDWI = (Band 3–Band 8)/(Band 3 + Band 8) following (Gao, 1996).

The above-mentioned independent variables were subsequently used to study how environmental factors affect the fractionation ratios of the REEs distribution in respect to the different landforms related to specific lithologies. In the present work, we do not provide a classification of landform types ("*objects*") but we quantify the land-surface using geomorphometric attributes (Schmidt and Dikau, 1999).

Therefore, we used a combined two-stage machine learning approach able to handle smaller sizes of sampled data (Yu et al., 2022; see also Supplementary Data file: Geostatistical modelling). The number of observed data i.e. REEs composition in topsoil and olive drupe in the study area was small (N = 85), which results in difficulties for the training of advanced deep learning models to obtain more accurate prediction results. To solve this problems, a two-stage approach was used to predict the spatial distribution of REEs taking into account the small samples size as follows: (1) The Multiple Regression Analysis (Bahrenberg et al., 1992; SAGA GIS software) was used to predict the spatial distribution of REEs in soil and olive drupe based on the sample data obtained and combined with environmental co-variables such as TWI, CND, etc., reported in the Supplementary Material (see Appendix A2); (2) The Stochastic Gradient Boosting (SGB - Friedman, 2002; Salford Predictive Modeler) was applied to assess the variable importance of the terrain-geology-olive drupe relationship and explore the relative influence of different environmental drivers on the fractionation ratio of La/Sm and La/Yb in topsoil and olive drupes.

Individual SGB models were performed for La/Sm and La/Yb. Moreover, also the sensitivity of the chosen parameters was assessed. The SGB models help to understand: (i) which environmental variables affect the distribution of REE in the soils of the olive groves, (ii) how topographical, geochemical and hydrological variables are linked (geodiversity) and (iii) how REE ratios vary in olive drupes according to the geodiversity: REEs absorbed by the roots of the olive trees and translocated towards the drupes (biodiversity).

The performance of the MARS models is reported in the Supplementary Material (see Appendix A3) and the evaluation of the REEs spatial distribution results was carried out using a multi-criteria approach: i) using a linear regression technique for the modelled value ratios of La/Sm and La/Yb (Fig. 3**e-f**) and ii) by Pearson's product-moment matrix correlation for modelled La/Sm and La/Yb (Table 1).

3. Results

3.1. Geochemistry of REE in the topsoil and in the olive drupes

The concentrations of REEs in the DTPA-bioavailable topsoil fractions showed differences between the lithologies with a range of the median value concentration of REEs (∑REEs) between 0.91 in claystone- (APA) and 22.08 ppm in sandstone – (MAC) derived soils.

The median value concentration of REEs (∑REEs) in olive drupes range between 1.11 in conglomeratic- and 18.20 ppb in sandstone-derived soils. The soil–plant transfer factor (SPTF), hence the ratio of the content of REEs in plants (olive fruit) to the content of REEs in soil (bioavailability) range from 1.0 10^{-4}–2.7 10^{-3} for conglomeratic- and flysh carbonatic-derived soils, respectively.

The range of different topsoil REE pattern generated in this study is shown in Fig. 2**a**.

According to the Oddo-Harkins rule (Rudnick and Fountain, 1995), REEs with even atomic numbers are always more abundant than their adjacent REEs. Various shape aspects of REE patterns were described quantitatively with normalized UCC (Upper Crust Continental) element ratios (Wedepohl, 1995), hereafter denoted by subscript N, and plotted in logarithmic scale (Fig. 2). A negative cerium (Ce) anomaly was identified for sandstones (MAC, siliciclastic turbidite) and a positive Ce anomaly for limestones (PTF, quartz-calcareous sandstones), marls, conglomerates (VILa) and basalts. No Eu peak was identified in any of the soils. The mafic intrusive and basaltic units displayed flat REE patterns, with general depletion. The ultramafic volcanic units had similar depleted Light-REE (LREE) values but higher Heavy-REE (HREE) values.

The olive drupe-REE patterns were characterized by positive Eu anomalies (Fig. 2**b**). The results show that Eu was preferentially mobilized from soil to olive drupe, due to its great affinity with Ca. The anomalous redox behavior of Eu explains its concentration in Ca-rich minerals, most notably in sedimentary lithotypes with respect to ophiolitic or basaltic outcrops of the Greve basin.

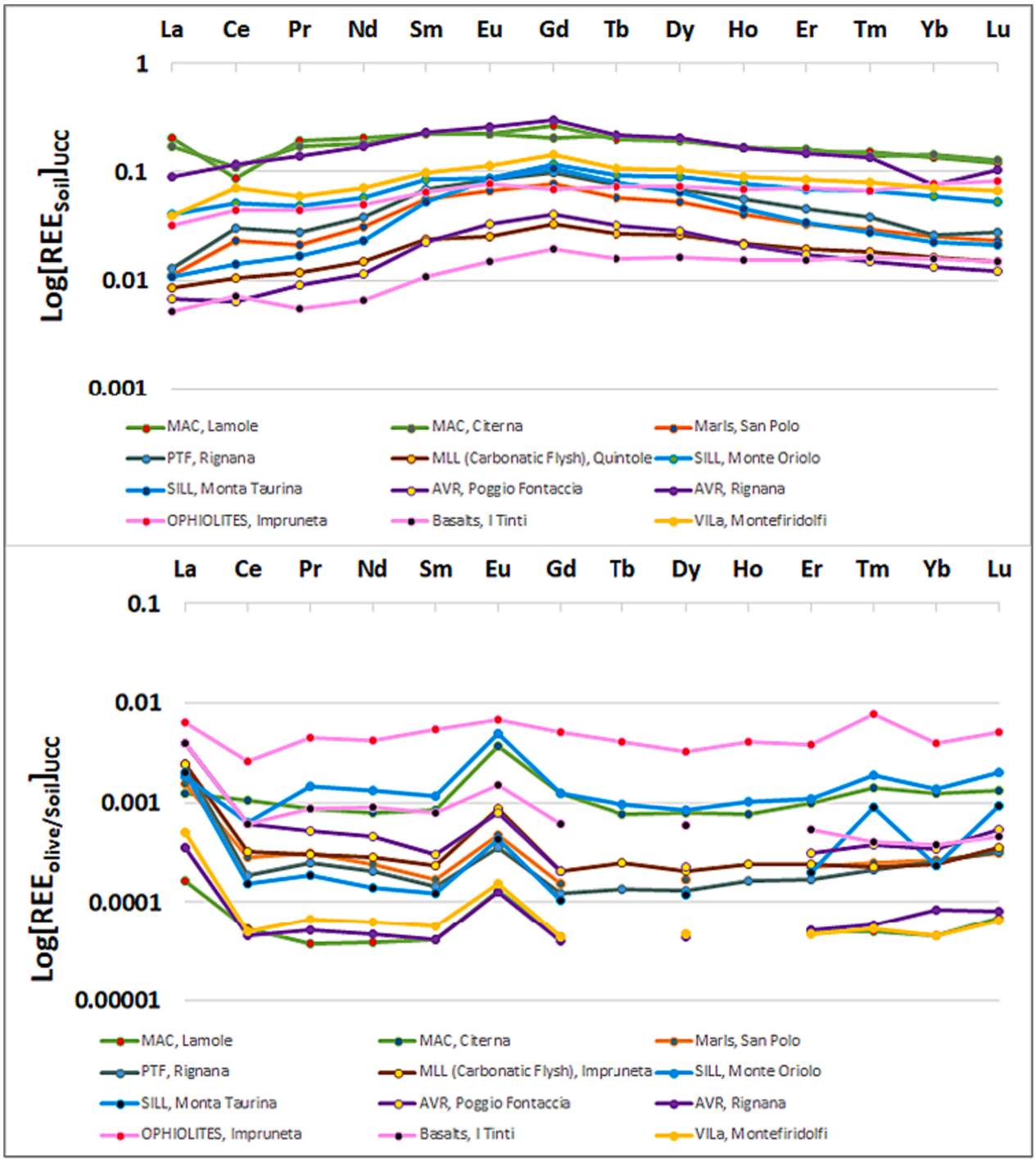

Fig. 2. (**a**) UCC-normalized REE fractionation patterns, in logarithmic scale, of bioavailable fraction in twelve topsoil for Chianti olive groves, Florence, Italy. Values below unity represent depletion with respect to Upper Continental Crust (UCC). The acronyms are referred to lithology (Fig. 1b; supplementary Tab. A1) and next the location of the olive grove. (**b**) The soil – REE normalized patterns of olives. Unlike the absolute concentrations, the sequences of normalized patterns were always independent by cultivar.

3.2. REEs abiotic-biotic signature

The interaction between organisms and their substrates that in turn supply nutrients modifies the balances of mobilized elements by preferential dissolution and absorption. The composition of elements therefore can be captured as fingerprint of the environment. Our results of abiotic La/Sm *vs.* La/Yb (topsoil) show surprisingly consistent behavior among the studied substrates and biota (olive drupe) finding a power law with a scaling relationship of 0.71 versus 0.83, respectively for soil and olive drupe (Fig. 3**c-d**).

The strongest signals were observed in basalts, ophiolites and claystone (APA) with a respective power law equation between topsoil and olive drupe (Fig. 3**a-b**). A decreasing power law was found in marls and arenaceous marls from topsoil to drupe, with exponent value of 1.6 to 0.9 and 1.3 to 0.6, respectively. The scaling exponent shows a steeper slope of 0.55 to 0.83 for claystone (chaotic body rock, SILL) and a slope of 0.44 to 0.83 for arenaceous derived soils.

Fig. 3**a** shows that the topsoil can be separated into four major

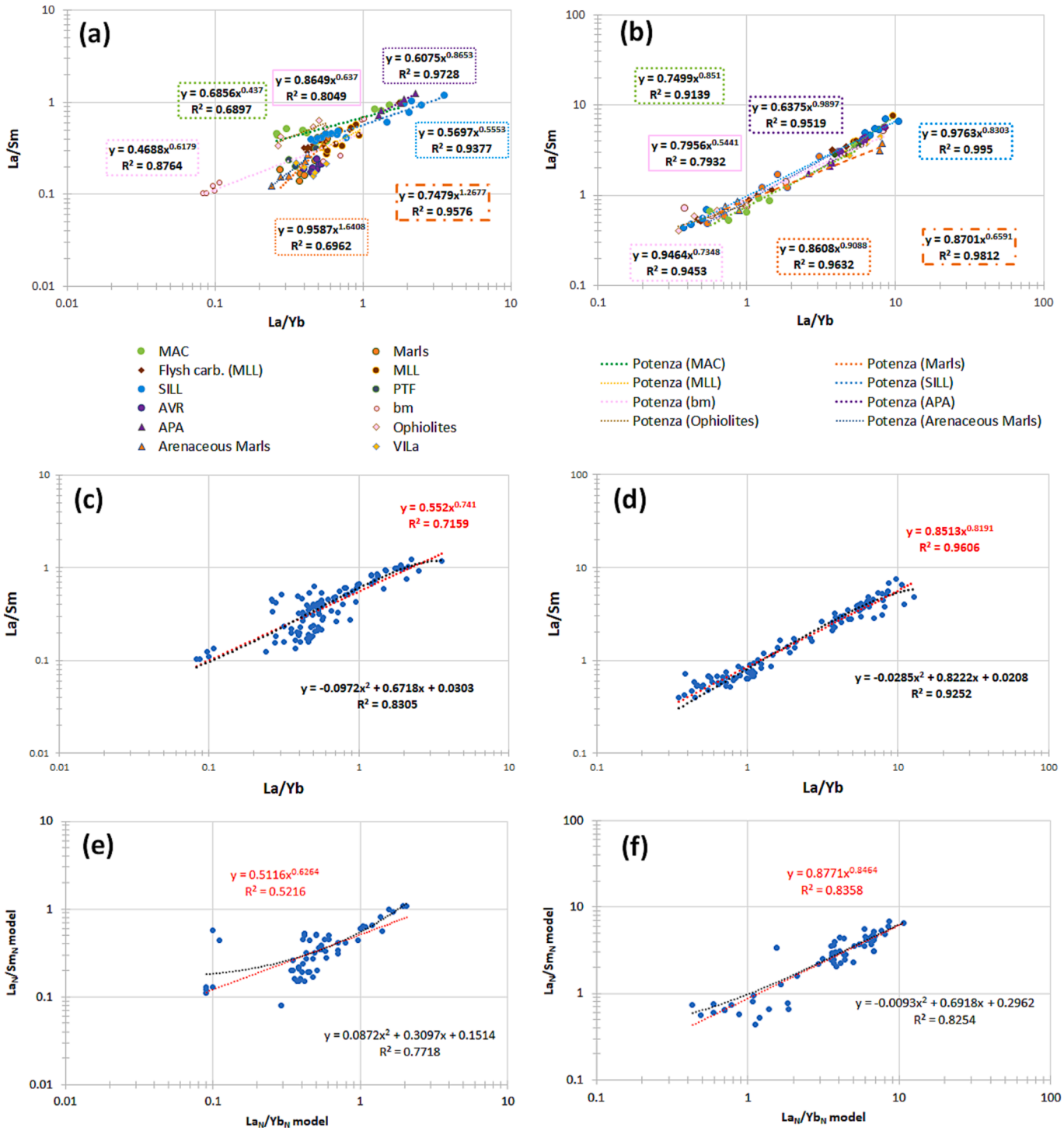

Fig. 3. REE fractionation patterns, [La /Yb] *vs.* [La/Sm] in logarithmic scale, for DTPA-bioavailable fraction of topsoil and olive drupe for Chianti area, fitted by a power law and a second order of polynomial function. The statistics as power law functions for contrasting parent material (different colors) considering topsoil and olive fruits are highlighted in (a) and (b), respectively. The general trends of all datasets are reported in (c) and (d), the slope of the relationships is −0.71 (not different from −3/4) for bioavailable REEs in topsoil and −0.83 for REEs translocated in the olive fruit. The values of La/Sm *vs.* La/Yb fractionation found by using MARS model referred to the sampling points are repoted in (e) and (f). A second degree polynomial function is also reported in (c)-(f).

categories: i) soil with a higher La_N/Sm_N and La_N/Yb_N ratio such as APA, SILL and MAC; ii) soils with low La_N/Sm_N and La_N/Yb_N ratio such as basalt – bm; iii) soils with low La_N/Sm_N and medium La_N/Yb_N ratio like AVR, Marls, Arenaceous marls, PTF and VILa; and iv) soils with medium La_N/Sm_N and La_N/Yb_N ratio such as MAC, ophiolites, MLL, Carbonatic Flysh and SILL.

The fractionation ratios showed that the plants grow on soils derived from ophiolites and basalts had a lower La_N/Sm_N and La_N/Yb_N ratio for olive drupes. On the contrary those grown on soils derived from APA and MLL had higher values. Instead SILL and MAC showed higher or medium to low values depending on the specific site (Fig. 3**a**).

Table 1
In 1a Pearson's product-moment matrix correlation for **measured** La/Sm and La/Yb REEs fractionation ratio, lithological, geomorphometric parameters, and hydrological characteristics in the Chianti study area, Tuscany, Italy. Note: La/SmO and La/YbO are referred to the olive drupe; in **1b** Pearson's product-moment matrix correlation among **modelled** covariate **with MARS:** La_N/Sm_N and La_N/Yb_N REEs fractionation ratio, lithological, geomorphometric parameters, and soil hydrological characteristics in the Chianti study area, Tuscany, Italy. Note: La/SmO and La/YbO are referred to the olive drupe.

1a

	La/Sm	La/Yb	La/SmO	La/YbO	CNBL	CND	VD	TWI	SLOPE	ASPECT	TRI	TPI	GEO	LS_F	NDWI	NDVI
La/Sm	1.00000															
La/Yb	0.87867	1.00000														
La/SmO	-0.16929	-0.07585	1.00000													
La/YbO	-0.14512	-0.05178	0.81581	1.00000												
CNBL	0.65213	0.66951	-0.41267	-0.36372	1.00000											
CND	-0.11430	-0.23207	0.20035	0.16757	-0.08082	1.00000										
VD	0.19303	0.21951	-0.32739	-0.20720	0.30977	-0.17620	1.00000									
TWI	0.25723	0.15285	0.11844	-0.00329	0.00560	-0.03692	-0.00419	1.00000								
SLOPE	0.37389	0.43108	-0.39560	-0.26550	0.51625	-0.29554	0.61159	-0.28446	1.00000							
ASPECT	0.21543	0.24907	0.06343	0.10755	0.20149	-0.08031	0.05336	-0.05848	0.26376	1.00000						
TRI	0.37842	0.43128	-0.40147	-0.27258	0.52799	-0.29168	0.62828	-0.29091	0.99813	0.26510	1.00000					
TPI	-0.44985	-0.40892	0.18442	0.25304	-0.27077	0.30155	-0.23072	-0.63239	-0.34469	-0.13397	-0.34280	1.00000				
GEO	0.36288	0.39600	0.11937	0.11727	0.25635	-0.33859	0.33650	0.01553	0.41629	0.22627	0.40384	-0.13271	1.00000			
LS_F	0.42909	0.46206	-0.39641	-0.29123	0.53173	-0.31313	0.70291	-0.09661	0.96960	0.26224	0.97327	-0.49092	0.40354	1.00000		
NDWI	-0.49428	-0.34003	0.20567	0.14559	-0.45645	0.10109	-0.47301	0.01622	-0.46425	-0.10322	-0.46955	0.15663	-0.58969	-0.49291	1.00000	
NDVI	0.52287	0.36703	-0.23566	-0.17473	0.44238	-0.15671	0.45219	0.00729	0.48020	0.05123	0.48383	-0.22236	0.62178	0.50360	-0.97873	1.00000

1.0000	0.7500	0.5000	0.2500	0	-0.2500	-0.5000	-0.7500	-1.0000

1b

	GEO	TWI	LS_F	CND	VD	TRI	CNBL	SLOPE	ASPECT	NDWI	NDVI	La/Sm	La/Yb	La/SmO	La/YbO
GEO	1.00000														
TWI	0.01791	1.00000													
LS_FACTOR	0.01973	-0.04735	1.00000												
CND	-0.07425	-0.35804	0.05768	1.00000											
VD	-0.02644	0.32021	0.25407	-0.56622	1.00000										
TRI	0.01591	-0.37556	0.91949	0.17927	0.11905	1.00000									
CNBL	-0.19882	0.00974	0.26057	0.11231	0.24337	0.22924	1.00000								
SLOPE	0.07918	-0.36296	0.71714	0.27877	-0.08567	0.81392	0.09398	1.00000							
ASPECT	-0.00878	-0.00894	0.01740	-0.02450	0.03561	0.02100	0.03569	-0.04499	1.00000						
NDWI	-0.16490	0.00168	0.00356	-0.04821	0.04979	-0.00888	-0.00330	-0.00182	0.02159	1.00000					
NDVI	0.17064	0.03796	0.03276	0.04661	-0.00750	0.02883	0.01553	-0.00009	0.00483	-0.91110	1.00000				
La/Sm	-0.05098	0.48646	0.05849	0.11106	-0.06362	-0.10528	0.65875	-0.11604	-0.00136	-0.37468	0.36156	1.00000			
La/Yb	0.10595	-0.08340	0.16833	0.17915	-0.00758	0.18916	0.67365	0.15305	-0.02611	-0.10725	0.10090	0.54990	1.00000		
La/SmO	0.33663	-0.02924	-0.36804	0.42119	-0.30565	-0.34939	0.02327	-0.36161	0.00264	0.39046	-0.43762	0.01324	0.19272	1.00000	
La/YbO	0.32038	-0.00041	-0.38551	0.29474	-0.26992	-0.37581	-0.12661	-0.36809	-0.00009	0.51725	-0.57776	-0.14832	0.02472	0.95586	1.00000

3.3. Importance of environmental variables for the terrain-geology relationship

To test whether local and landscape environmental heterogeneity characteristics affect REEs distribution both in soils and olive drupes, we applied a stochastic gradient boosting approach (SGB). We use the SGB model to assess the variable importance and hence, to reduce complexity selecting the most important variables. The results were highlighted in Fig. 4.

The variable importance provides understandings into the most relevant environmental information dominating the different landforms (geodiversity) of the Greve watershed (Fig. 4). Results of the SGB model, where the terrain covariates plus NDVI and NDWI are the independent variables and the lithotypes the target variable, show that channel network base level (CNBL), valley depth (VD) and vertical distance to channel network (CND) are the most important variables to predict the variation of landform geodiversity in the Greve watershed (Fig. 4-**a**). NDVI, NDWI, LS- factor, Aspect, Terrain Ruggedness Index (TRI), Slope and Topographic Wetness Index (TWI) are less important accounting for forty percent of importance in respect to CNBL, which is the most important covariate in predicting the thirteen lithologies characterizing the Greve basin (Fig. 1, Fig. 4).

If we consider only the spatial distribution of the olive groves, the results show a general agreement with the landforms model applied for the entire basin even if some differences are noted (Fig. 4-**a**). The predictors VD, CND, ASPECT, and TWI show a higher importance for the spatial distribution of olive grove in respect to the model computation for the entire basin.

Furthermore, the two variable partial dependence plots (PDP, Fig. 5) allow insights on the interactions of the covariates. The PDP of TWI and CNBL for olive groves growing on PTF and Marls are reported in Fig. 5.

The two PDP show how TWI and CNBL influences the prediction while averaging with respect to all the other features of a machine learning model (Friedman, 2001). A flat PDP with lower log odd indicates that the feature is not important, and the more the PDP varies, the more important the functionality. For olive groves on Marls, we

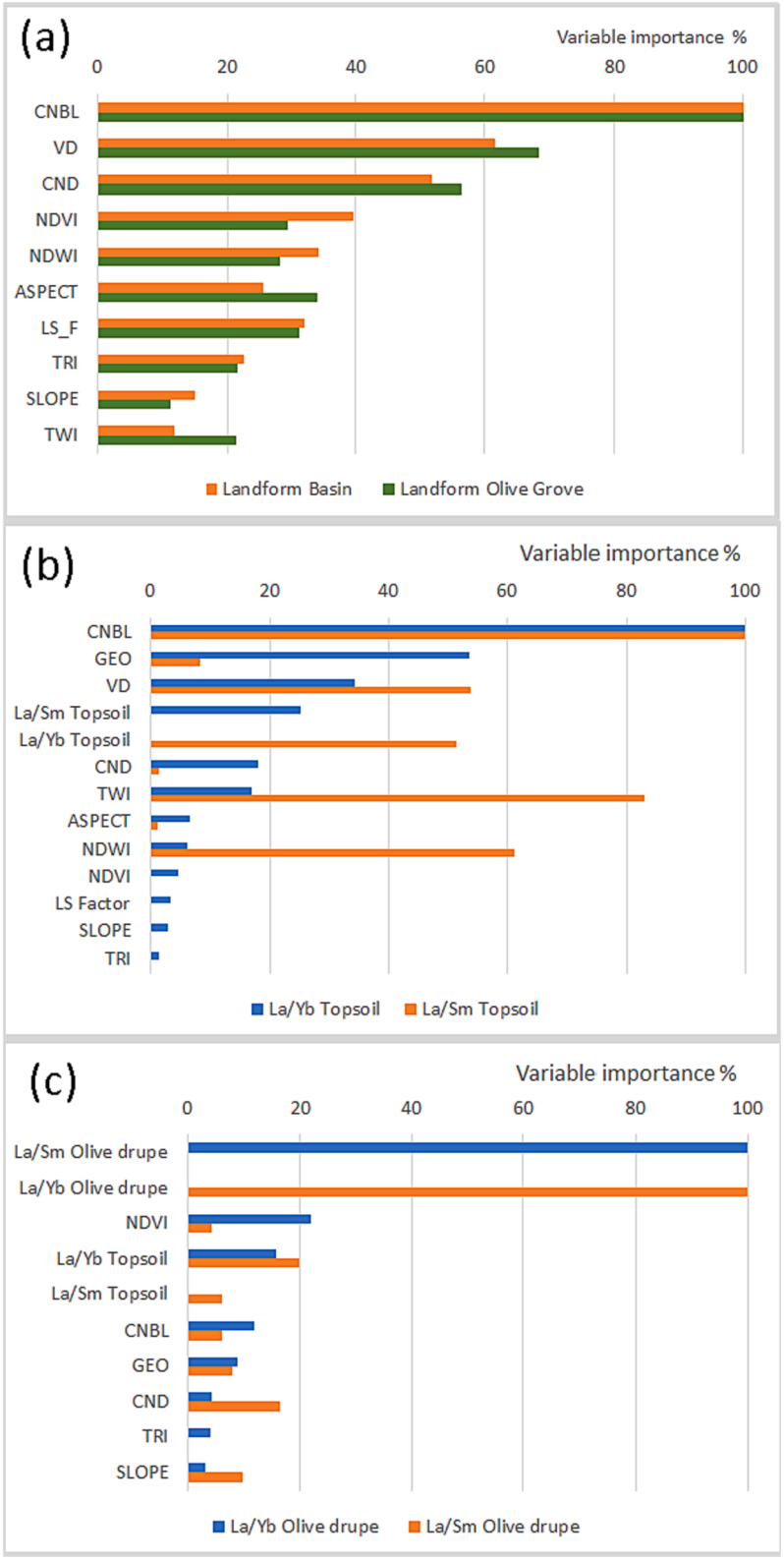

Fig. 4. Variable importance calculated for SGB in relation to the most important predictor for the spatial distribution of: (**a**) the lithotypes for the Greve watershed, Florence, Tuscany, Italy, considering terrain predictors, NDVI and NDWI for the basin and for only olive grove land use; (**b**) La/Sm and La/Yb fractionation ratios for topsoil and (**c**) La/Sm and La/Yb fractionation ratios for olive drupe. The variables are expressed in decreasing order and normalized to 100%; (**d**) Importance values of the landforms conditioning factors for nine contrasting lithologies related to olive grove in Chianti area, Florence, Tuscany, Italy. Legend: Channel Network Base Level (CNBL), Valley Depth (VD), Vertical Distance to Channel Network (CND), Terrain Ruggedness Index (TRI), Topographic Index (TPI), Topographic Wetness Index (TWI), Normalized Difference Vegetation Index (NDVI) and Normalized Difference Water Index (NDWI).

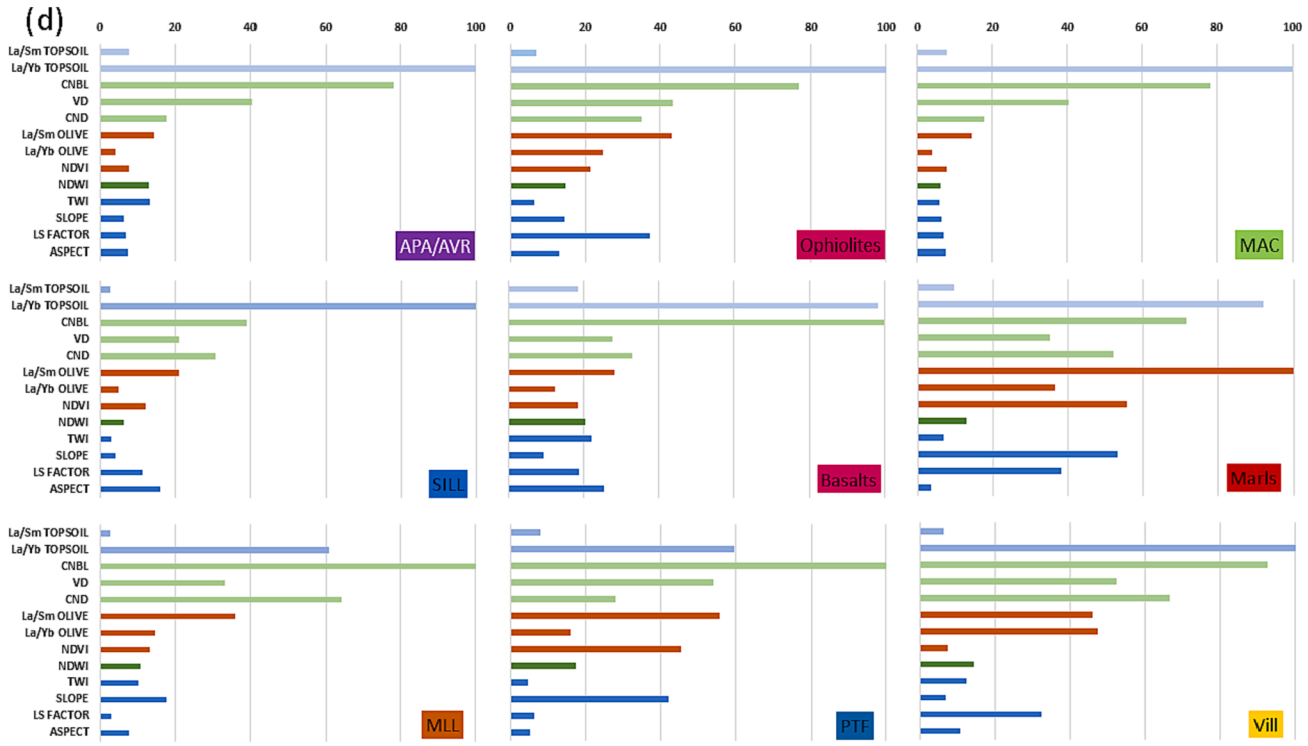

Fig. 4. (*continued*).

observed a step- pool pattern with a positive value of log odd ratios (or probability ratio) related to values of CNBL varying from 275 m to 594 m and TWI varying from 5 to 15 (Fig. 5 **EO**). Interesting, if the model is applied on the basin scale we lose the information of the spatial distribution of the anthropically graded terraces that characterized the olive groves (Fig. 5**E2**). The same conclusion can be drawn for the PTF outcropping (Fig. 5**B**).

3.4. Assessment of REEs distribution—Environmental heterogeneity relationship

The correlations between the landform covariates and the REEs fractionation ratios in olive groves were firstly evaluated using the Pearson's product-moment matrix for the 85 analyzed sampling points, located in 17 different olive groves **(**Table 1**a)**. Our results show that for topsoil the determined fractionation ratio La/Sm and La/Yb are mainly related to CNBL. Furthermore, a significant negative correlation between NDVI and NDWI was found, and these two biophysical variables show a different coefficient of correlation with the lithology, +0,62 *vs.* −0.59, respectively. The same behavior was found in topsoil for the fractionation values of La/Sm, that are negatively correlated to NDWI and positively to NDVI.

We modelled the spatial distribution of La_N/Sm_N and La_N/Yb_N, for (i) olive groves, 22 % of the basin and (ii) for the entire Greve basin. Model (i) was used to assess the statistics hence the variable importance (Fig. 4b-d) and the correlation between factors (Table 1b), whereas model (ii) reflects a scenario analysis for REEs distribution at basin scale (Fig. 6).

The spatial distributions results of La_N/Sm_N and La_N/Yb_N at basin scale using the Multiple Regression Analysis model are shown in Fig. 6 and the respective performance criteria in Supplementary Data (**Annex A3**).

The correlation between the cofactors and the spatial distribution of La_N/Sm_N and La_N/Yb_N was evaluated using Pearson's product-moment matrix. As illustrated in Fig. 3e-f and Table 1b the values are reproducing those obtained by the measured values.

The maps presented in Fig. 6 only considered olive groves and thus do not reflect other land use. The four maps (Fig. 6) highlight how the fractionation ratio in topsoil and olive drupe is differently distributed.

Higher values of La_N/Sm_N in topsoil ($La_N/Sm_N > 1.0$) are mainly distributed in the southern and eastern parts of the Greve basin characterized by arenaceous rocks and along the hydrological network. In general the La_N/Sm_N ratio of topsoil shows a decreasing value according to the elevation ranges, whereas, as a shown in Fig. 4**b**, the interrelation of only a few abiotic landscape factors characterize the topsoil distribution of La_N/Sm_N such as CNBL, TWI, NDWI, VD and CND. All topographic indices show a variable importance of more than 50 %, indicating a well-defined relationship of these REEs ratios with the hydrological and geomorphological characteristics of the landscape.

The low values of La_N/Yb_N in topsoil ($La_N/Yb_N < 1.0$) are mainly distributed in the central parts of the basin and in the north-western parts, indicating that the fractionation ratio between the LREE and HREE was significant lower in these parts of the basin compared to the upper and the eastern parts. As reported in Fig. 4**b** the La_N/Yb_N ratio is stronger correlating with CNBL, lithology (GEO), VD and less with La/Sm topsoil, CND and TWI.

Considering the spatial distribution of La_N/Sm_N and La_N/Yb_N in the olive drupe (Fig. 6**c-d**), we are aware that the model was conducted only for olive groves. However, the variability highlighted the same lithological differences. The low values of La_N/Sm_N are mainly distributed in the middle and western parts of the basin where serpentinite crops out as well as in the eastern parts where marls are dominant. In general as shown in Fig. 4**c** the distribution of La_N/Sm_N and La_N/Yb_N in the olive drupe is strongly related to the La_N/Yb_N in topsoil compared to La_N/Sm_N in the topsoil. Higher values of La_N/Yb_N (>5.0) in the olive drupe are mainly found in the lower and eastern parts of the basin (Fig. 6**d**). Conversely, in the western parts we found values lower than 5. In general, the ratio La/Sm in olive drupe is stronger correlated to La/Yb olive drupe, followed by topsoil La/Yb (account 20 %) and CND. Olive drupe La/Yb is less correlated to slope, GEO, CNBL and NDVI. The variables contributing to the La/Yb olive drupe model where olive drupe La/Sm is followed by NDVI (more than 20 %), topsoil La/Yb, CNBL and CND. The

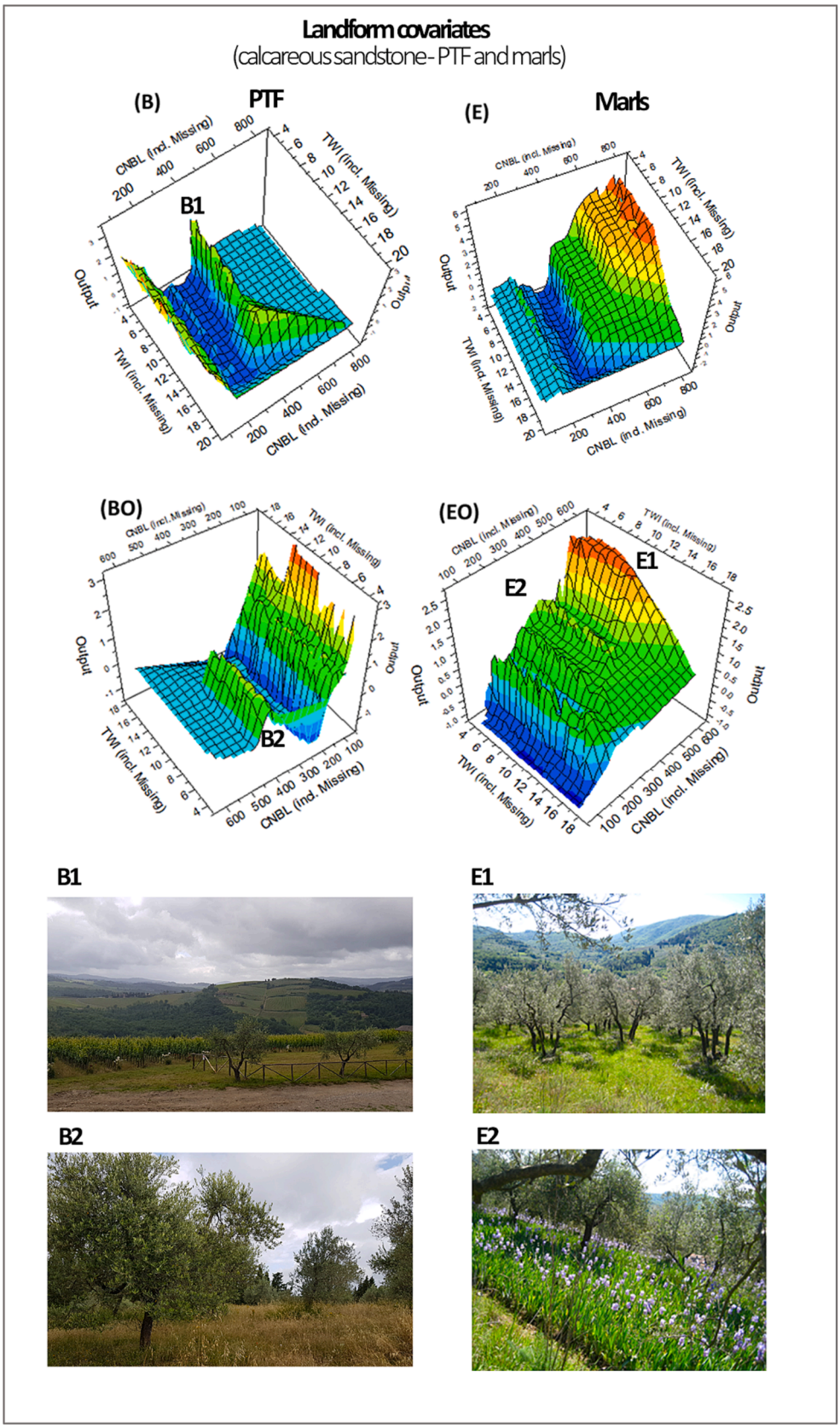

Fig. 5. Two-variable dependence plots for Channel Network Base Level (CNBL) and Topographic Wetness Index (TWI) were shown for PTF (B) and Marls (E) outcropping in the Greve basin, Florence, Italy. The BO and EO were referred to spatial distribution of olive groves. For the SGB model we used the terrain covariates as predictor and the geology as target variable. The four taken pictures highlighted the good performance of the model. E1 and E2 photos refer to olive groves on marl and how their topographic and hydrological characteristics can be identified and therefore explained with the SGB model, in particular by the two cofactors TWI and CNBL (EO). B1 and B2 photos refer to the different land uses occupying the upper part of the slope characterized by the calcareous sandstone (PTF).

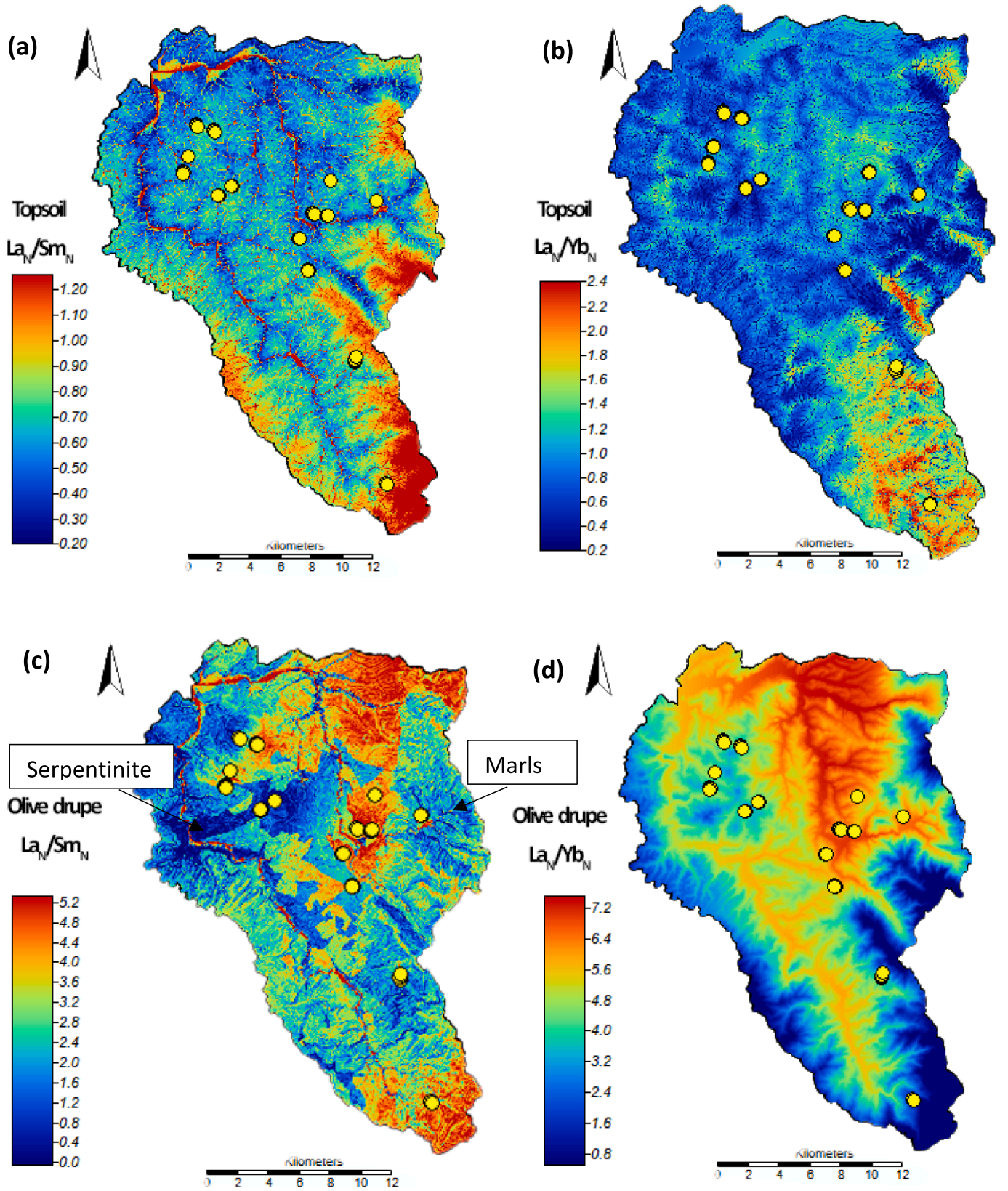

Fig. 6. Multiple Regression Analyses model results of La/Sm(A), La/Yb(B) spatial distribution characteristics for topsoils and La/Sm(C), La/Yb(D) for olive drupe in Chianti area, Greve basin, Florence, Italy.

NDWI factor shows no contribution to biotic REEs ratios (Fig. 4**c**).

Furthermore, results showed that the response of La/Sm to NDVI change followed an S-shaped curve (Fig. 9a). In contrast, the PDP of the La/Yb and NDVI had a linear trend (Fig. 9b). The La/Sm plots show that the relative importance of NDVI decreases with an increase in the negative curvature values and an increase in flattening, corresponding to NDVI values ranging from 0.1 to 0.554. Conversely, the La/Yb plots show an increasing relative importance moving from NDVI values of 0.532 to 0.1. We noted that the NDVI has moderate to low values with increasing La/Yb ratio.

Focusing on the single target variable, hence on landforms developed on specific lithologies, the SGB model results (classification) show that bio-geodiversity relationships are related to each lithology for the single covariates taken into consideration. Fig. 4**d** illustrates the importance values revealing the factors influencing the landforms for nine contrasting lithologies. We observed that the topographic covariate slope and LS-factor are the most correlated with olive drupe La/Sm and secondly to the olive drupe La/Yb, especially for the lithotypes Marls, Vill, PTF, ophiolites and to a minor degree for MLL. Furthermore, the ratio La/Yb of the topsoil is the most important predictor for all landform lithotypes, in respect also to La/Sm, but except for MLL and PTF where the CNBL shows an importance value of 100 %. On the other hand, the biotic factor represented by the olive drupe La/Sm ratio is an important covariate showing higher importance values than La/Yb in many landform lithotypes.

4. Discussions

4.1. Environmental factors and their effects on the spatial distribution of topsoil REEs fractionation ratio

Landform diversity influences and interacts with both biodiversity and geodiversity. Hence, it is a key factor in improving landscape resilience. Quantification of morphology and its recognition is important to understand its formation and evolution mechanism (Jasiewicz and Stepinski, 2013; Martins et al., 2016). In this study, we investigated the effects of topography on the spatial distribution of La/Sm and La/Yb, Light-REE/Medium-REE and L-REE/Heavy-REE, in different topsoils of Tuscany olive groves. The SGB model results indicate as most relevant environmental information dominating the different landforms of the Greve watershed the channel network base level (CNBL), followed by valley depth (VD) and vertical distance to channel network (CND), the latter accounting for 56 % in respect to CNBL (Fig. 4**a**).

The influence of these topographic features on the predicted lithologies is illustrated in Fig. 7.

Interestingly the response curve (RC) for eight different landform lithotypes show a negative contribution of the CNBL model in the range of 270–400 m (Fig. 7**a**). Furthermore, the different parent materials have different transition points in CNBL. For instance, the CNBL curves for calcareous siltstone (PTF) showed a positive contribution with different intensities of RC at 400 m and in the range of 100–270 m. These results suggest that channel network and valley depth have a major role in driving soil distribution and landscape evolution in the Chianti study

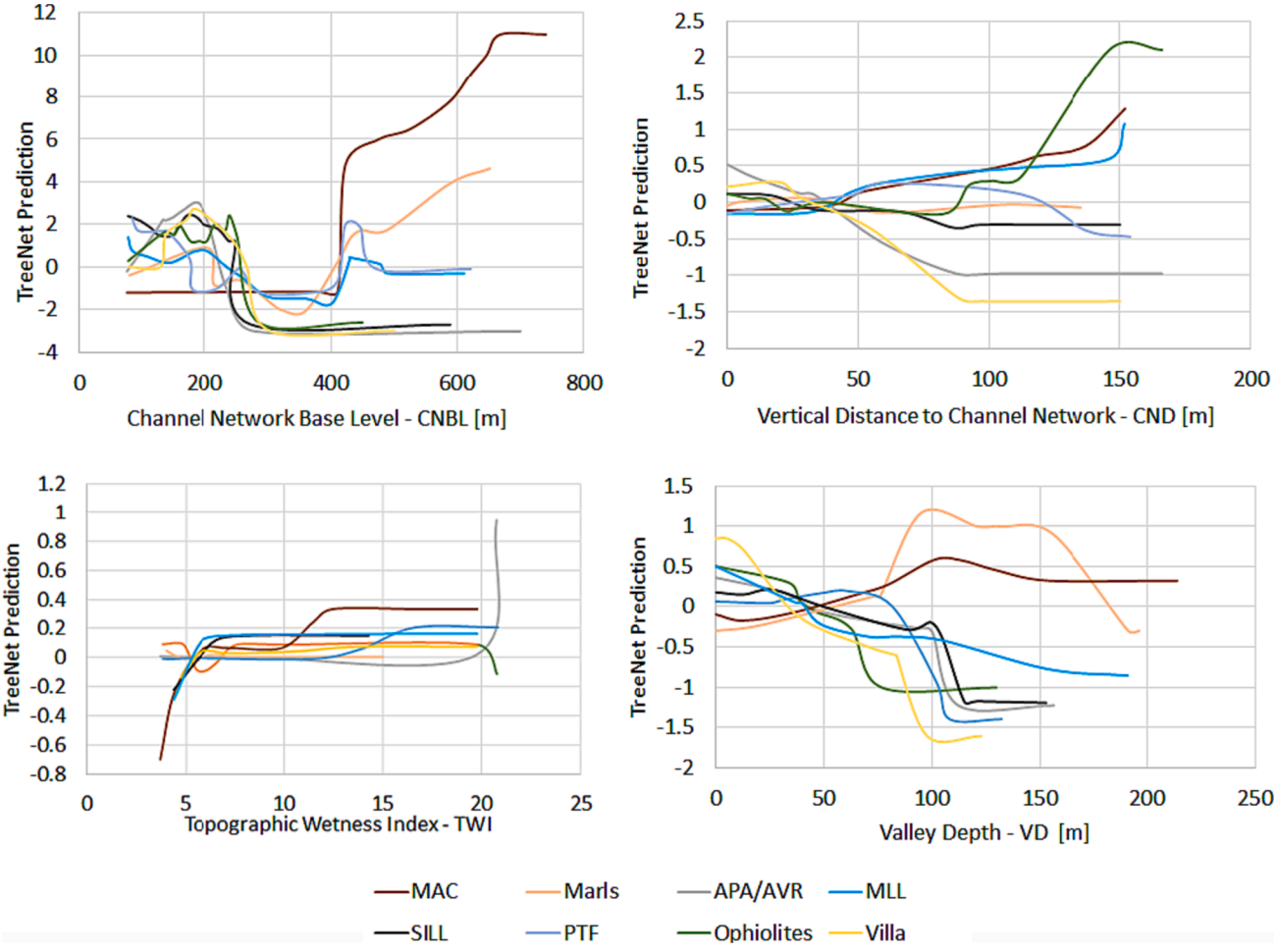

Fig. 7. Single variable partial dependence plots (PDP) for the three most important variable predictor (CNBL, CND, VD) and Topographic Wetness Index (TWI) of landform geodiversity SGB model for Chianti area.

area through runoff and discharge as well as weathering processes. On the other hand, the primary factor of the landscape evolution of this basin is tectonic controls followed by the different denudation rates that affect the contrasting lithologic substrates. This underpins that tectonic activity is the main driver of landscape evolution where a rapid rate of isostatic uplift has modified the hydrological systems through a 3.6 Ma years chronosequence (Cornamusini et al., 2011).

These results appear to be consistent with those reported in literature, where surface elevation is regarded as the most common variable and important of many topographic parameters used in digital soil mapping (McBratney et al., 2003; Sahragarda and Pahlavan-Rad, 2020). Youssef and Doumit (2022) showed that the Valley depth (VD) index increases proportionally with the erosion threshold and is either climate or tectonically dependent. Fig. 7**d** reports the RC for VD, showing that marls are highly sensitive in the range of 70–100 m, with an increasing positive slope, and between 150 and 190 m with a negative slope. MAC shows a peak at VD value equal to 110 m. Paleo-fluvial conglomerate outcrops show a peak at VD value of 10 m and can be clearly distinguished from claystone (APA/AVR), limestones (MLL) and ophiolites showing a lower response for low VD values.

Elevation also controls the patterns of runoff generation or saturation excess overland flow and the velocity of runoff (Huang et al., 2002; Jencso and McGlynn, 2011). In line with these findings, it was stated that elevation plays a remarkable role in the soil erosion processes and soil solute transport and hence on distribution and fractionation of REEs (Ma and Rate, 2009; Yuan et al., 2021). Nonetheless, contrasting findings were reported by different studies (Song et al., 2017; Yuan et al. 2021), authors generally agree with the fact that the LREE are more mobile and preferentially exported by surface and subsurface runoff, and more available for root absorption than HREE (Brioschi et al., 2013). These findings are confirmed by the fact that TWI and NDWI were important covariates in topsoil La_N/Sm_N ratio variation in the study area (Fig. 4**b,** Fig. 6). Conversely, the main control on the distribution of La_N/Yb_N in the topsoils (LREE/HREE) is the parent rock material, as illustrated in Fig. 4**b.** Lithology accounts for 53.7 % compared to CNBL. Our results highlighted that the topsoil La_N/Yb_N ratio is a major covariate for all landform lithotypes with the exception for MLL and PTF (Fig. 4**d).** This might be explained by the calcareous nature of these soils where HREEs generally show a higher bioavailability and mobility than LREEs. In accordance with these findings, it was shown by Song et al. (2017) that HREEs values decreased with elevation in a Triassic limestone hillslope. Considering the western side of the Greve basin, the limestone formation shows decreasing values of the topsoil La_N/Yb_N ratio compared to e.g. PTF outcrops. (Fig. 4**d** – PTF). Furthermore, Xinde et al. (2000) show that the bioavailability of different REEs varied due to the soil exchangeable fractions and carbonate bounds.

4.2. Environmental variables affecting the distribution of REEs in the olive drupe

Our study examines the relationships between topsoil REE fractions and olive plant REE uptake considering the REE present in the olive drupe. As shown in Fig. 2**b** our findings are in line with previous studies demonstrating that the distribution patterns of REEs in olive drupes follow the composition of REEs in the soil, indicating that olive trees in pomace do not accumulate or selectively assimilate REEs with the exception of europium (e.g. Pošćić et al., 2020, Barbera et al., 2022), lanthanum and cerium (Fig. 8).

Consequently, the soil signal or soil fingerprint in terms of the REE composition is reported also for the respective olive drupes for most elements (Fig. 2**b**).

The La anomaly in environmental samples is still poorly understood. However, recent studies highlighted that biological activity can fractionate LREE (e.g., Hibi et al., 2011; Pol et al., 2014; Semrau et al., 2018; Barrat et al., 2023). In our study area the olive drupe cultivated on soils derived from conglomerate, limestone, claystone, and carbonate rocks, showed an positive anomaly of La ($La/La^* > 3$) and hence, a higher fractionation of La/Yb (>2.6). Lanthanum is essential for some functional groups in specific ecosystems where the methanol dehydrogenase enzymatic activity of bacteria is involved to oxidize methanol to produce energy (Hibi et al., 2011; Picone and den Camp, 2019). Wang et al. (2020) reported positive La anomalies in methanotrophic mussels probably due to microbial enzymatic activity related to aerobic methane oxidation. The latter suggests that the La anomaly could be used as a diagnostic tool for tracing past biological activity related to aerobic methanotrophy. For olive trees, Anguita-Maeso et al. (2020) showed that the *Methylobacterium* was one of the most representative genera in the xylema sap of the plant. In this regard, recent bioinformatic techniques highlighted that many microbial phyla and genera in soil and in the xylema sap of the plant are related to the enrichment and fractionation of REEs (Anguita-Meso et al., 2021; Li et al., 2022). Since many questions remain open regarding the fractionation of HREEs, Eu anomaly (e.g. Ding et al., 2006) and Ce anomaly during the translocation from the rhizosphere to the aerial parts of the plant, more scientific studies regarding the chemical and microbial characterization of the xylema sap are needed.

Furthermore, the typical REEs concentrations in olive drupe are in the order of ppt. Thus, spectral interferences on the REE analysis, such as $^{135}Ba^{16}O^+$ and $^{137}Ba^{16}O^+$ on $^{151}Eu^+$ and $^{153}Eu^+$, and $^{138}BaH^+$ on $^{139}La^+$, might lead to an overestimation of their concentrations (e.g. Pourret et al., 2022). To overcome this problem the most appropriate analytical approach should be taken into consideration (Wysocka, 2021).

In the present research we followed an analytical procedure described in the material and method section, that should have removed the polyatomic interferences but, as mentioned before, some question remain open, especially to explain the Eu positive anomaly detected in olive drupe (Fig. 8c), which need further investigation beyond the scope of the present study.

Interestingly a negative Ce anomaly was found in the olive drupe, especially in those cultivated on ophiolites-derived soils in agreement with the study conducted for different shrub and perennial herbaceous plant species collected in an arid area of Oman (Semhi et al., 2009). The negative Ce anomaly in olive drupe ranges from 0.61 for olive groves on ophiolites to 0.96 for quartz-calcareous siltstones (PTF) with an insignificant Ce anomaly. There were also olive drupes where Ce anomaly is absent, as for olive groves on conglomerates (VIL) or slightly positive for fine limestone/marly limestones (MLL) and basalts (named I Tinti). Other authors reported that the negative Ce anomaly in plants is due to the fact that Ce in soil can assume a valence of +4 reducing the plant availability or uptake (Brookins, 1989; Wyttenback et al., 1998). Pošćić et al. (2017) related the Ce depletion in plant tissue to the biochemical reaction in root symplast with a formation of precipitate of $CePO_4$, that limited the aboveground translocation. The Ce and Eu anomaly is generally explained through changes of their valence state under different redox conditions, making them different from other REEs (+3). Our results showed that a depletion of Ce was found in arenaceous soils (MAC) and related olive drupes (Fig. 8B). This behavior was previously reported in weathered soils on granites (Middelburg et al., 1988). Pédrot et al. (2015) related the soil solution Ce anomaly signature to the topographic variability in the organic carbon (OC)/Fe(Mn) ratio, and found a relationship between a low OC/Fe ratio and the negative Ce anomaly. This is in agreement with our results, where the arenaceous soils (MAC) are characterized by a lower soil organic carbon content (SOC) equal to 0.54 % and a higher Fe content of 131 mg/kg in respect to the other olive orchard with a medium SOC value of 1.5 % and Fe = 28 mg/kg. Furthermore, a positive Ce anomaly was found in calcareous soils characterized by ferromanganese oxides in agreement with previous studies (Zhou et al., 2020).

Considering the olive grove of the Greve watershed, for the REE pattern in soil and olive drupe, a power law relationships where found reported in Eq. (1):

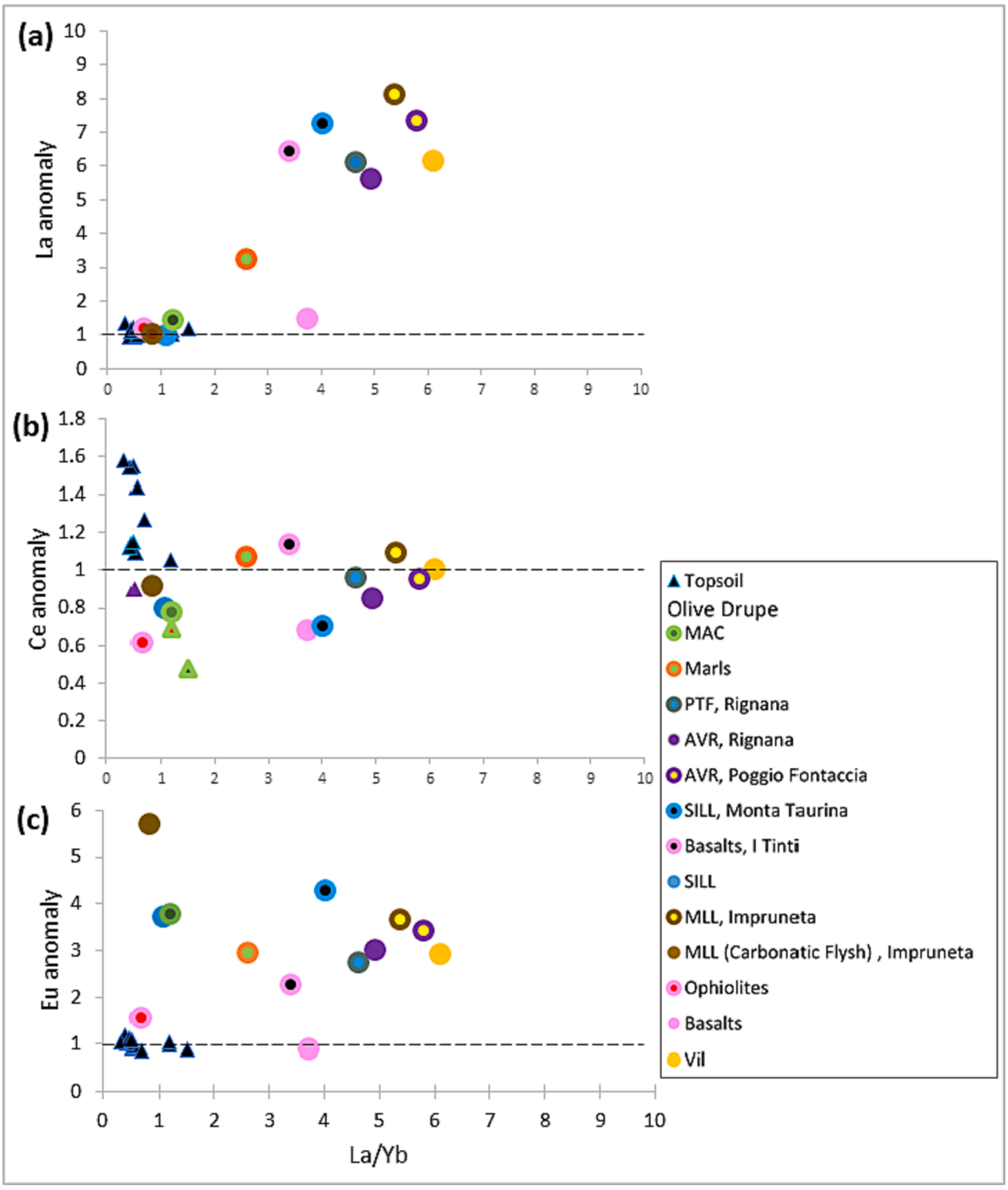

Fig. 8. (a) La/La* *vs.* La_N/Yb_N diagram. The ratio La/La* (calculated as $La_N/[(Pr_N)^3/(Nd_N)^2]$; Barrat et al., 2023) is a measure of the size of the lanthanum anomaly normalized to UCC (N) abundance of La relative to Pr and Nd. A significant positive lanthanum anomaly (La/La* > 1) in a olive drupe is regarded as evidence related to biological activity (Barrat et al., 2023). (b) Ce/Ce* *vs.* La_N/Yb_N diagram. The ratio Ce/Ce* (calculated as $Ce_N/[(Pr_N)^2/(Nd_N)]$; Barrat et al., 2023) shows that the Macigno formation samples (arenaceous soils, green color triangles) are on average more depleted in Ce than other samples. (c) Eu/Eu* *vs.* La_N/Yb_N diagram shows a significant positive europium anomaly (Eu/Eu* > 1) in olive drupes. This is regarded as an evidence that could indicate that Eu^{2+} replace Ca^{2+} in plant tissues (Zeng et al., 2003). A lower Eu anomaly was found in olive drupes cultivated on ophiolites and basalts (Eu/Eu* < 1) (Impruneta district, serpentinite outcrop see Fig. 6c). The ratio Eu/Eu* is calculated as $Eu_N/(Sm_N \times Gd_N)^{0.5}$ (McLennan and Taylor 2012). (For interpretation of the references to color in this figure legend, the reader is referred to the web version of this article.)

$$Y = ax^b \quad (1)$$

Where Y is a response or dependent variable (La/Sm), x represents an independent or explanatory variable (La/Yb), α is a normalization constant and b is the scaling exponent.

The element accumulation pattern in the drupe of olive plants under organically management showed a scaling relationship with a power law equal to 0.8 for the fractionation ratios of La/Sm *vs*. La/Yb, that can be considered as an enrichment in MREEs or HREEs (=depletion in LREEs). A comparable value of b close to 3/4 was obtained for the universal power law of metabolism (Savage et al., 2004; Marquet et al., 2005; Glazier, 2014). An equivalent pattern in respect to the drupe was found for the bioavailable fraction of topsoil, showing a scaling factor equal to 0.7 (Fig. 3**c–d**). These findings represent the internal dynamics of the systems and suggest that plant mechanisms are regulating the REE translocation from the rhizosphere to the olive drupe following different pathways (Fig. 3**a–b**). The latter depends on different abiotic factors such as the rock mineralogy as well as the element content in soils or the characteristics of particular species. We hypothesize that the interaction between rock, water and biota (plant and microbial communities) determines the variability patterns of REEs (see Zaharescu et al., 2017). Furthermore, the accumulation of elements in the olive drupe of the different geochemical environments of the study area show a comparable path, highlighting how the dynamics also depend on the values of the ionic radii and valences of the element (Alekseenko et al., 2021). LREE partitioning is specific for plant species (Brioschi et al., 2013; Kovaříková et al., 2019; Ramos et al., 2016; Wyttenbach et al., 1998). In terms of the olive drupe the enrichment or depletion of the MREE values in respect to HREE values (La/Sm *vs* La/Yb) show a scale exponent b with values between 0.54 and 0.99, respectively for ophiolites and claystone.

Considering the ratios of La/Yb in the western part of the basin, we noticed that the spatial model for olive drupes (Fig. 6D) better approximated the REEs variation within the basin and are in line with the graphical representation shown in Fig. 8a (positive La anomaly). The western part of the Greve basin is dominated by ophiolitic complexes (Brizzi and Meli, 1996) characterized by montmorillonitic soils (Malquori and Cecconi, 1956). The olive drupes growing on these soils (SILL, carbonatyc flysh and ophiolites) show the lowest values in the La_N/Yb_N ratios close to 1 (0.98–1.16) and no La anomaly. Consequently, we can state that REEs can trace the pedogenetic processes from different parent rock material especially considering non-polluted soils (Laveuf and Cornu, 2009).

Many researchers have previously shown evidence that both soil and landscape are complex systems showing fractal properties (e.g., Rodriguez-Iturbe et al., 1996; Ibáñez et al., 2009; Phillips, 2013; San-José and Caniego, 2013). Phillips (1998) demonstrated that the equation of soil forming factors (Jenny, 1941) can be solved and understood in the framework of non-linear dynamical systems theory. Non-linear and complex systems are the product of the interactions between the diverse elements that characterize the system such as the drainage basin structure, landforms and regolith, among many others (Rodriguez-Iturbe et al., 1996; Philips, 2003). Taking this into account, the interaction between spatial heterogeneity and diversity are the driving forces for the emergence of complex systems (Dolson et al., 2017; Pettersson and Jacobi, 2021). The results obtained for the La/Sm and La/Yb spatial distribution models, based on the interaction of the terrain and lithological covariates, reflecting the soil formation factors, show the link between the topographic, geochemical and hydrological variables (geodiversity) and therefore, how this might change the response of the biotic components (REE accumulation pattern in olive drupe). The enrichment/depletion of HREE in the topsoil affect more the distribution pattern of the La_N/Sm_N and La_N/Yb_N ratios in olive drupe than the MREE. In our study area the enrichment/depletion of HREE in the topsoil is mainly affected by the terrain covariates CNBL and by the lithologies (Fig. 4). This general model for the Greve basin shows some particularities according to the landform lithotypes as shown in Fig. 4**d**.

Given the importance of the remote-sensing-based biophysical indicators such as NDVI in the spatial prediction of La/Yb in olive drupe, we further investigated the variable relationships between these co-predictors (Fig. 9). In recent years, a number of studies focused on monitoring of land cover change especially in the REE mining areas using NDVI (e.g., Xie et al., 2020). For the study area, the NDVI has a maximum value of 0.9 for areas with very high active photosynthetic vegetation and a value of 0.1 for areas with low activity. Hence, a spatial difference in the biomass production can be observed. These findings are in line with Ott (2020) who showed that vegetation associated to siliciclastic, plutonic and metamorphic rocks exhibits elevated value of NDVI in contrast to carbonate areas. Hence, reflecting lithologic variations in soil nutrients and hydrology that promote or inhibit habitat suitability. For instance, soils developed on carbonate rocks (karst regolith) are more susceptible to drought (Jiang et al., 2020) and have lower nutrient content than other rocks (Porder and Ramachandran, 2013; Tyler, 1996). Jiang et al. (2020) pointed out the role of limestone bedrock geochemistry in affecting vegetation activity by regulating the critical zone (CZ) water holding capacity. This is matching with our results showing that the NDVI values represent an importance value of 45 % and 55 % for spatial prediction of PTF and Marls lithologies, respectively.

5. Conclusion

Our research represents a starting point for future applications and modelling techniques to analyze at catchment-scale the REEs biophysical fluxes and food traceability. The aim of this study has been to understand the spatial distribution of REEs in soils and olive drupes and their relationship to describe catchment-scale biophysical fluxes. In this context, we show that the use of the fractionation ratio La/Sm *vs.* La/Yb is a powerful ecological index to evaluate and monitor the system dynamic and the related evolutionary trends at basin level. Particularly, the proposed method yields valuable information to evaluate the impacts of REEs on the environment and the respective organisms. This study set the basis to provide a holistic assessment of the toxicity level of an ecosystem. Integrated studies like this are important to identify critical processes that can cause secondary toxicity throughout the food chain (see also Tibbett et al., 2021). On the other hand, this research also contributes to the valorization of a healthy food product. In conclusion, our study illustrates that bedrock geochemistry influences plant growth and hence, also the quality of the final product (drupes and Olive oil). This specific relation between bedrock and vegetation is documented by the variable importance of NDVI and La/Yb in olive drupes. Despite the uncertainties regarding the role and fate of some LREE (La, Eu and Ce), the proposed approach provides valuable insights into the functioning of terrestrial ecosystems that are determined by a wide range of processes with complex interactions across the biosphere, pedosphere and lithosphere. All these components need to be considered to obtain a full and detailed picture of any studied terrestrial ecosystem. Future research will focus on the study of the interactions between microbial endophytic and LREEs to investigate in particular the development of La anomalies as well as a wide range of land uses. The assessment of the latter allows for a better understanding of the bio-chemical fluxes of REEs at the catchment scale. Overall, our research highlighted that the contents of REEs (La/Sm and La/Yb) in the olive drupe were successfully predicted with the DTPA-bioavailable topsoil fractions of REEs and terrain features using machine learning techniques. However, further verifications with other olive drupe varieties and soil types should be carried out in future.

Funding

Financial support provided by Rural Development 2014–2020 for Operational Groups (in the sense of Art 56 of Reg.1305/2013) Tuscany

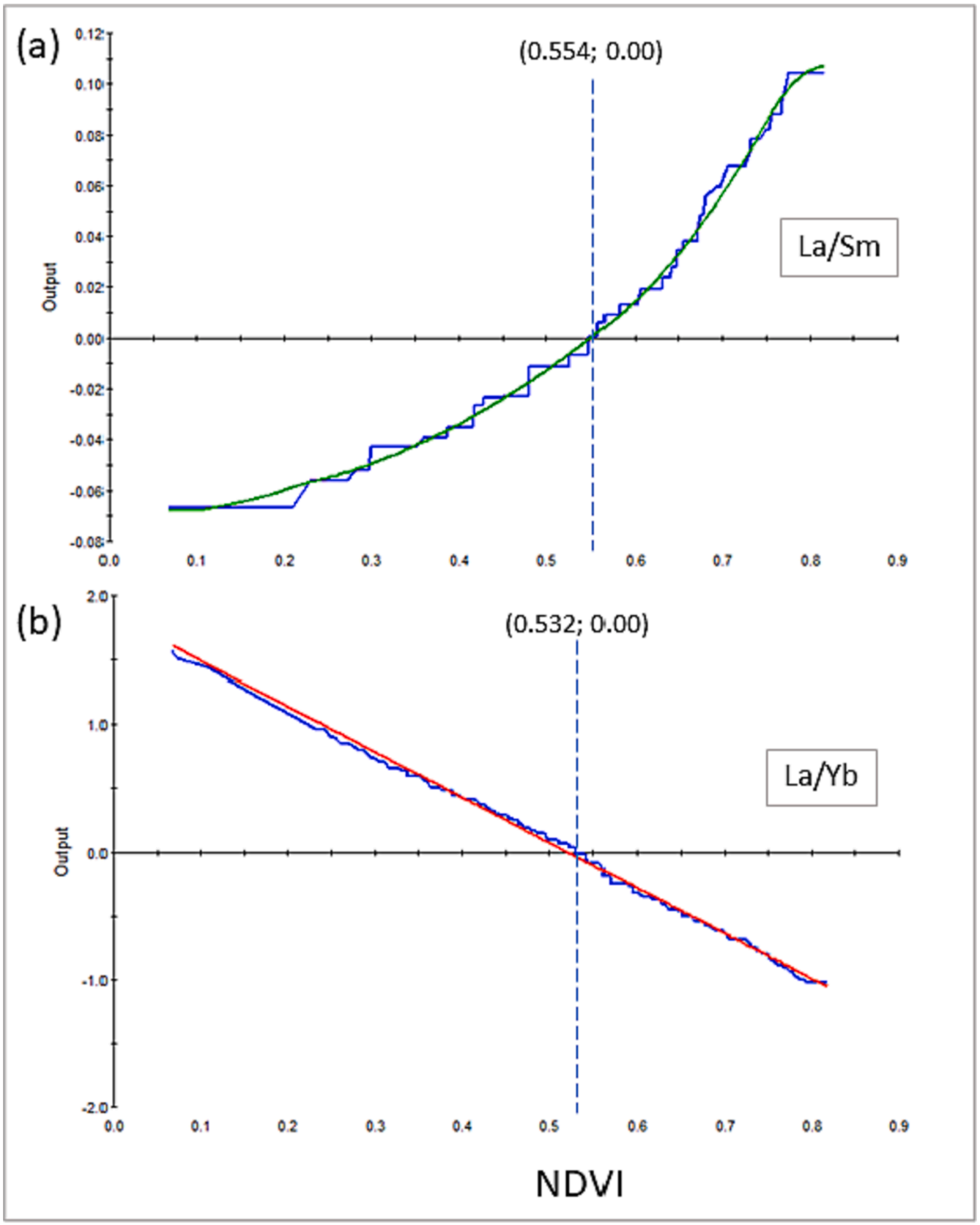

Fig. 9. Single variable partial dependence plots (PDPs) for La/Sm ratio (a) and La/Yb ratio (b) related to NDVI as biophysical predictor. Partial dependence is the effect that a predictor has predicting the dependent variable, when all other predictors in the model are set to their mean value. The x-axis shows the full range of values of the predictor variable (NDVI). The y-axis shows the backwards log transformation of a log-odd to produce a probability metric for a presence prediction for the La/Sm ratio (a) or the La/Yb ratio (b).

Region, through the Project GeOEVO-App "Enhancement of extra virgin olive oil through geographical traceability and product characterization".

CRediT authorship contribution statement

Samuel Pelacani: Conceptualization, Formal analysis, Investigation, Writing – original draft, Writing – review & editing. **Michael Maerker:** Methodology, Supervision, Writing – review & editing. **Simone Tommasini:** Formal analysis, Investigation, Methodology, Writing – review & editing. **Sandro Moretti:** Funding acquisition, Supervision, Writing – review & editing.

Declaration of competing interest

The authors declare that they have no known competing financial interests or personal relationships that could have appeared to influence the work reported in this paper.

Data availability

The data are available as Supplementary Material

Acknowledgments

The authors are thankful for the contribution of the owners and farm technicians of Chianti area, Dr. Clemente Pellegrini Strozzi, Dr. Ovidio Mugnaini, Dr. Filippo Legnaioli, Dr. Paolo Socci, Cosimo Gericke and Gionni Pruneti for their collaboration and support of the fieldwork. Furthermore, we would like to thank you for their support in the REE analyses Dr. Roberto Riccio, Dr. Andrea Malpaganti and Dr. Cristiano Pucci.

Appendix A. Supplementary data

Supplementary data to this article can be found online at https://doi.org/10.1016/j.ecolind.2024.111583.

References

Adeniyi, O.D., Brenning, A., Bernini, A., Brenna, S., Maerker, M., 2023. Digital mapping of soil properties using Ensemble Machine learning approaches in an agricultural lowland area of Lombardy, Italy. Land 12 (2), 494. https://doi.org/10.3390/land12020494.

Aide MT & Aide C (2012) Rare Earth Elements: Their Importance in Understanding Soil Genesis. ISRN Soil Science Volume 2012, Article ID 783876, 11 pages doi:10.5402/2012/783876.

Alekseenko, et al., 2021. Element accumulation patterns of native plant species under the natural geochemical stress. Plants 10 (1), 33. https://doi.org/10.3390/plants10010033.

Alexander, C., Deák, B., Heilmeier, H., 2016. Micro-topography driven vegetation patterns in open mosaic landscapes. Ecol. Ind. 60, 906–920.

Anderson, M.G., Ferree, C.E., 2010. Conserving the stage: Climate change and the geophysical underpinnings of species diversity. PLoS One 5, e11554.

Anguita-Maeso, M., Olivares-García, C., Haro, C., Imperial, J., Navas-Cortés, J.A., Landa, B.B., 2020. Culture dependent and culture-independent characterization of the olive xylem Microbiota: Effect of sap extraction methods. Front. Plant Sci. 10, 1708. https://doi.org/10.3389/fpls.2019.01708.

Anguita-Maeso, M., Haro, C., Montes-Borrego, M., De La Fuente, L., Navas-Cortés, J.A., Landa, B.B., 2021. Metabolomic, ionomic and microbial characterization of olive xylem sap reveals differences according to plant age and genotype. Agronomy 11 (1179). https://doi.org/10.3390/agronomy11061179.

Bahrenberg, G., Giese, E., Nipper, J., 1992. Statistische Methoden in der Geographie 2 - Multivariate Statistik. Stuttgart, p. 415p.

Bailey, J.J., Boyd, D.S., Hjort, J., Lavers, C.P., Field, R., 2017. Modelling native and alien vascular plant species richness: At which scales is geodiversity most relevant? Glob. Ecol. Biogeogr. 26, 763–776.

Barbera, M., Saiano, F., Tutone, L., Massenti, R., Pisciotta, A., 2022. The pattern of rare earth elements like a possible helpful tool in traceability and geographical characterization of the soil-olive system (Olea europaea L.). Plants 11, 2579.

Barbera, M., Zuddas, P., Piazzese, D., Oddo, E., Lopes, F., Censi, P., Saiano, F., 2023. Accumulation of rare earth elements in common vine leaves is achieved through extraction from soil and transport in the xylem sap. Commun. Earth Environ. 4, 21. https://doi.org/10.1038/s43247-023-00950.

Barrat, J.A., Bayon, G., Lalonde, S., 2023. Calculation of cerium and lanthanum anomalies in geological and environmental samples. Chem. Geol. 615, 121202.

Bertoldi, D., Larcher, R., Nicolini, G., Bertamini, M., Concheri, G., 2009. Distribution of rare earth elements in Vitis vinifera L. 'Chardonnay' berries. Vitis J. Grapevine Res. 48, 49–51.

Brierley, G., Fryirs, K., Jain, V., 2006. Landscape connectivity: the geographic basis of geomorphic applications. Royal Geographical Society 38 (2), 165–174.

Brioschi, L., Steinmann, M., Lucot, E., Pierret, M.C., Stille, P., Prunier, J., Badot, P.M., 2013. Transfer of rare earth elements (REE) from natural soil to plant systems: implications for the environmental availability of anthropogenic REE. Plant Soil 366, 143–163. https://doi.org/10.1007/s11104-012-1407-0.

Brizzi, G., Meli, R., 1996. I minerali della formazione ofiolitica dell'Impruneta (FI). Riv. Miner. Ital. 20 (1), 81–98.

Brookins, D.G., 1989. Aqueous geochemistry of rare earth elements. In: Lipin, B.R., McKay, G.A. (Eds.), Geochemistry and Mineralogy of Rare Earth Elements. Mineralogical Society of America, Washington, DC, pp. 201–226.

Catrouillet, C., Guenet, H., Pierson-Wickmann, A.C., Dia, A., LeCoz, M.B., Deville, S., Lenne, Q., Suko, Y., Davranche, M., 2019. Rare earth elements as tracers of active colloidal organic matter composition. Environ. Chem. 17 (2), 133–139. https://doi.org/10.1071/EN19159.

Censi, P., Saiano, F., Pisciotta, A., Tuzzolino, N., 2014. Geochemical behaviour of rare earths in Vitis vinifera grafted onto different rootstocks and growing on several soils. Sci. Total Environ. 473–474, 597–608.

Chen, W.J., Tao, Y., Gu, Y.H., Zhao, G.W., 2001. Effect of lanthanide chloride on photosynthesis and dry matter accumulation in tobacco seedlings. Biol. Trace Elem. Res. 79, 169–176.

Conrad, O., Bechtel, B., Bock, M., Dietrich, H., Fischer, E., Gerlitz, L., Wehberg, J., Wichmann, V., Böhner, J., 2015. System for Automated Geoscientific Analyses (SAGA) v. 2.1.4. Geosci. Model Dev. 8, 1991–2007. https://doi.org/10.5194/gmd-8-1991-2015.

Cornamusini, G., Ielpi, A., Bonciani, F., Callegari, I., Conti, P., 2011. Thrusting, strike-slip tectonics and stratigraphic architecture in a thrust-belt belt (Chianti Mts, Northern Apennines). Soc. Geol. It. 15, 47–50.

Dauphin, et al., 2023. Re-thinking the environment in landscape genomics. Trends Ecol. Evol. 38, 3.

De Falco, N., Berger, R.T., Hjazin, A., Yizhaq, H., Stavi, I., Rachmilevitch, S., 2021. Geodiversity impacts plant community structure in a semi-arid region. Sci. Rep. 11, 15259.

Ding, S., Liang, T., Zhang, C., Huang, Z., Xie, Y., Chen, T., 2006. Fractionation mechanisms of rare earth elements (REEs) in hydroponic wheat: an application for metal accumulation by plants. Environ. Sci. Technol. 40, 2686–2691. https://doi.org/10.1021/es052091b.

Dolson, E.L., Perez, S.G., Olson, R.S., Ofria, C. (2017) Spatial resource heterogeneity increases diversity and evolutionary potential. https://doi.org/10.1101/148973.

Fazzini, P., Gelmini, R., 1982. Tettonica trasversale nell'Appennino Settentrionale. Soc. Geol. Ital. Mem. 24, 299–309.

Festa, A., Pini, G.A., Dilek, Y., Codegone, G., 2010. Mélanges and mélange-forming processes: a historical overview and new concepts. Int. Geol. Rev. 52 (10–12).

Friedman, J.H., 2001. Greedy function approximation: A gradient boosting machine. Ann. Stat. 1189–1232.

Friedman, J.H., 2002. Stochastic gradient boosting. Comput. Stat. Data Anal. 38, 367–378.

Gao, B.C., 1996. NDWI - A normalized difference water index for remote sensing of vegetation liquid water from space. Remote Sens. Environ. 58, 257–266.

Giles, T.P., 1998. Geomorphological signatures: classification of aggregated slope unit objects from digital elevation and remote sensing data. ESPL 23 (7), 581–594.

Glazier, D.S., 2014. Metabolic scaling in complex living systems. Systems 2 (4), 451–540. https://doi.org/10.3390/systems2040451.

Gray, M., 2021. Geodiversity: A significant, multi-faceted and evolving, geoscientific paradigm rather than a redundant term. Proc. Geol. Assoc. 132, 605–619.

Guisan, A., Weiss, S.B., Weiss, A.D., 1999. GLM versus CCA spatial modeling of plant species distribution. Plant Ecol. 143, 107–122.

Henderson P. (1984) Rare earth element geochemistry. In: *Developments in Geochemistry 2*. Elsevier, London, UK, 510pp.

Hibi, Y., Asai, K., Arafuka, H., Hamajima, M., Iwama, T., Kawai, K., 2011. Molecular structure of La3+-induced methanol dehydrogenase-like protein in Methylobacterium radiotolerans. J. Biosci. Bioeng. 111 (5), 547–549.

Hjort, J., Luoto, M., 2010. Geodiversity of high-latitude landscapes in northern Finland. Geomorphology 115, 109–116.

Huang, C., Gascuel-Odoux, C., Cros-Cayot, S., 2002. Hillslope topographic and hydrologic effects on overland flow and erosion. Catena 46 (2–3), 177–188.

Hunter, M.L., Jacobson, G.L., Webb, T., 1988. Paleoecology and the coarse-filter approach to maintaining biological diversity. Conserv. Biol. 2, 375–385.

Ibáñez, J.J., Brevik, E.C., 2022. Geodiversity research at the crossroads: two sides of the same coin. Span. J. Soil Sci. https://doi.org/10.3389/sjss.2022.10456.

Ibáñez, J.J., Pérez-Gómez, R., San José Martínez, F., 2009. The spatial distribution of soilsacross Europe: A fractal approach. Ecol. Complex. 6, 294–301.

Ibáñez, J.J., Ramírez-Rosario, B., Fernández-Pozo, L.F., Brevik, E.C., 2021. Exploring the scaling law of geographical space: Gaussian versus Paretian thinking. Eur. J. Soil Sci. 72, 495–509. https://doi.org/10.1111/ejss.13031.

Iwahashi, J., Pike, R.J., 2007. Automated classifications of topography from DEMs by an unsupervised nested-means algorithm and a three-part geometric signature. Geomorphology 86 (3–4), 409–440.

Jasiewicz, J., Stepinski, T.F., 2013. Geomorphons — a pattern recognition approach to classification and mapping of landforms. Geomorphology 182, 147–156.

Jencso, K.G., McGlynn, B.L., 2011. Hierarchical controls on runoff generation: Topographically driven hydrologic connectivity, geology, and vegetation. Water Resour. Res. 47, 11.
Jenny, H., 1941. Factors of Soil Formation: A System of Quantitative Pedology. McGraw-Hill, New York.
Jiang, Z., Liu, H., Wang, H., Peng, J., Meersmans, J., Green, S.M., Quine, T.A., Wu, X., Song, Z., 2020. Bedrock geochemistry influences vegetation growth by regulating the regolith water holding capacity. Nat. Commun. 11, 2392. https://doi.org/10.1038/s41467-020-16156-1.
Jucker, T., Bongalov, B., Burslem, D.R.F.P., Nilus, R., Dalponte, M., Lewis, S.L., Phillips, O.L., Qie, L., Coomes, D.A., 2018. Topography shapes the structure, composition and function of tropical forest landscapes. Ecol. Lett. https://doi.org/10.1111/ele.12964.
Kavvadias, V., Koubouris, G., 2019. Sustainable soil management practices in olive groves. Soil Fertility Manage. Sustain. Dev. 167–188.
Khan, A.M., Bakar, N.K.A., Bakar, A.F.A., Ashraf, M.A., 2017. Chemical speciation and bioavailability of rare earth elements (REEs) in the ecosystem: a review. Environ. Sci. Pollut. Res. 24, 22764–22789.
Kovaříková, M., Tomášková, I., Soudek, P., 2019. A review - Rare earth elements in plants. Biol. Plant. 63, 20–32.
Laush, A., et al., 2020. Linking the remote sensing of geodiversity and traits relevant to biodiversity—Part II: Geomorphology, terrain and surfaces. Remote Sens. 12 (22), 3690. https://doi.org/10.3390/rs12223690.
Laveuf, C., Cornu, S., 2009. A review on the potentiality of Rare Earth Elements to trace pedogenetic processes. Geoderma 154, 1–12.
Li, X., Liang, X., He, H., Li, J., Ma, L., Tan, W., Zhong, Y., Zhu, J., Zhou, M.F., Dongf, H., 2022. Microorganisms accelerate REE mineralization in supergene environments. Appl. Environ. Microbiol. 88 (13).
Liao, Y., Lu, P., Mo, D., Wang, H., Storozum, M.J., Chen, P., Xu, J., 2019. Landforms influence the development of ancient agriculture in the Songshan area, central China. Quat. Int. 521, 85–89.
Ma, Y., Rate, A.W., 2009. Formation of trace element biogeochemical anomalies in surface soils: the role of biota. Geochem. –Explor. Environ. Analysis 9, 353–367.
Maerker, M., Bosino, A., Scopesi, C., Giordani, P.G., Firpo, M., Rellini, I., 2020. Assessment of calanchi and rill-interrill erosion susceptibility in northern Liguria, Italy: A case study using a probabilistic modelling framework. Geoderma 371, 114367. https://doi.org/10.1016/j.geoderma.2020.114367.
Malquori, A., Cecconi, S., 1956. Minerali argillosi di terrenti provenienti da rocce ofiolitche. La Ricerca Scientifica 26, 1154–1159.
Märker, M., Pelacani, S., Schröder, B., 2011. A functional entity approach to predict soil erosion processes in a small Plio-Pleistocene Mediterranean catchment in Northern Chianti, Italy. *Geomorphology* 125 (4), 530–540.
Marquet, P.A., Quiñones, R.A., Abades, S., Labra, F., Tognelli, M., Arim, M., Rivadeneira, M., 2005. Review - Scaling and power-laws in ecological systems. J. Exp. Biol. 208, 1749–1769.
Martins, F.M.G., Fernandez, H.M., Isidoro, J.M.G.P., Jordán, A., Zavala, L., 2016. Classification of landforms in Southern Portugal (Ria Formosa Basin). J. Maps 12 (3).
McBratney, A.B., Mendoca Santos, M.L., Minasny, B., 2003. On digital soil mapping. Geoderma 117 (1–2), 3–52.
McFeeters, S.K., 1996. The use of the normalized difference water index (NDWI) in the delineation of open water features. Int. J. Remote Sens. Int. 17 (7), 1425–1432.
McLennan, S.M., Taylor, S.R., 2012. Geology, geochemistry, and natural abundances of the rare earth elements. Encyclopedia of Inorganic and Bioinorganic Chemistry. John Wiley & Sons Ltd.
Merla, G. (1969) - Macigno del Chianti. Studi Illustrativi della Carta Geologica d'Italia, Formazioni geologiche 2: 65-77, Roma.
Middelburg, J.J., van der Weijden, C.H., Woittiez, J.R.W., 1988. Chemical processes affecting the mobility of major, minor and trace elements during weathering of granitic rocks. Chem. Geol. 68 (3–4), 253–273.
Milne, G., 1936. Normal erosion as a factor in soil profile development. Nature 138 (3491), 548–549.
Montgomery, D.R., Zabowski, D., Ugolini, F.C., Hallberg, R.O., Spaltenstein, H., 2000. Soils, watershed processes, and marine sediments. Int. Geophys. 72, 159–194.
Parks, K.E., Mulligan, M., 2010. On the relationship between a resource based measure of geodiversity and broad scale biodiversity patterns. Biodivers. Conserv. 19, 2751–2766. https://doi.org/10.1007/s10531-010-9876-z.
Pascucci, V., Martini, I.P., Sagri, M., Sandrelli, F., 2007. Effects of transverse structural lineaments on the Neogene-Quaternary basins of Tuscany (inner Northern Apennines, Italy). In: Nichols, G., Paola, C., Williams, E.A. (Eds.), *Sedimentary Processes, Environments and Basins* – A Tribute to Peter Friend, vol. 37. IAS Spec. Pub, pp. 155–183.
Pédrot, M., Dia, A., Davranche, M., Gruau, G., 2015. Upper soil horizons control the rare earth element patterns in shallow groundwater. Geoderma 239–240, 84–96.
Pelacani, S., Tommasini, S., Ungaro, F., Falcone, E.E., & Saiano, F. (2017) Rare Earth Elements Analysis For Extra Virgin Olive Oil Assessment: The Case Study Of Tuscany Olive Groves, Italy. XXVI Congresso Nazionale della Società Chimica Italiana.
Perez Sanchez, A., Schibalski, A., Schroder, B., Klimek, S., Dauber, J., 2023. Local and landscape environmental heterogeneity drive ant community structure in temperate semi-natural upland grasslands. Ecol. Evol. https://doi.org/10.22541/au.165760390.06995388/v1.
Pettersson, S., Jacobi, M.N., 2021. Spatial heterogeneity enhance robustness of large multi-species ecosystems. PLoS Comput. Biol. https://doi.org/10.1371/journal.pcbi.1008899.
Philips, J.D., 2003. Sources of nonlinearity and complexity in geomorphic systems. Prog. Phys. Geogr.: Earth Environ. 27 (1).
Phillips, J.D., 1998. On the relations between complex systems and the factorial model of soil formation (with discussion). Geoderma 86, 1–21.
Phillips, J., 2013. Nonlinear Dynamics, Divergent Evolution and Pedodiversity. In: Ibáñez, J.J., Bockheim, J.G. (Eds.), Pedodiversity. CRC Press, Boca Raton, p. 256 pp..
Picone, N., den Camp, H.J.O., 2019. Role of rare earth elements in methanol oxidation. Curr. Opin. Chem. Biol. 49, 39–44.
Pike, R.J., 1988. The geometric signature: quantifying landslide-terrain types from digital elevation models. Math. Geol. 20 (5), 491–510.
Pol, A., Barends, T.R.M., Dietl, A., Khadem, A.F., Eygensteyn, J., Jetten, M.S.M., Op den Camp, H.J.M., 2014. Rare earth metals are essential for methanotrophic life in volcanic mudpots. Environ. Microbiol. 16, 255–264.
Porder, S., Ramachandran, S., 2013. The phosphorus concentration of common rocks—a potential driver of ecosystem P status. Plant Soil 367, 41–55.
Pošćić, et al., 2020. Accumulation and partitioning of rare earth elements in olive trees and extra virgin olive oil from Adriatic coastal region. Plant Soil 448, 133–151.
Pošćić, F., Schat, H., Marchiol, L., 2017. Cerium negatively impacts the nutritional status in rapeseed. Sci. Total Environ. 593–594, 735–744.
Pourret, O., van der Ent, A., Hursthouse, A., Irawan, D.E., Liu, H., Wiche, O., 2022. The 'europium anomaly' in plants: facts and fiction. Plant Soil 476, 721–728.
Rate, A.W. & Ma, Y. (2010) Formation of soil geochemical anomalies by plant uptake of trace elements. 19th World Congress of Soil Science, Soil Solutions for a Changing World 1 – 6 August 2010, Brisbane, Australia.
Riley, S.J., DeGloria, S.D., Elliot, R., 1999. A terrain ruggedness index that quantifies topographic heterogeneity. Intermt. J. Sci. 5 (1–4), 23–27.
Rodriguez-Iturbe, I., Marani, M., Rigon, R., Rinaldo, A., 1996. Self-organized river basin landscape: Fractal and multifractal characteristics. WRR 30 (12), 3531.
Rouse, J., Haas, R., Schell, J., Deering, D., 1973. Monitoring vegetation systems in the great plains with ERTS. Third ERTS Symposium, NASA. 1, 309–317.
Rudnick, R., Fountain, D., 1995. Nature and composition of the continental-crust—a lower crustal perspective. Rev. Geophys. 33 (3), 267–309.
Ruhe, R.V., Walker, P.H. (1968) Hillslope models and soil formation.1. Open systems. In: Transactions of the 9th International Congress on Soil Science (Adelaide, SA: 1968); Int.Soil Sci.Soc.and Angus And Robertson Sydney. Vol.4:551-60.
Sahragarda, H.P., Pahlavan-Rad, M.R., 2020. Prediction of soil properties using random forest with sparse data in a semi-active volcanic mountain. Eurasian Soil Sci. 53 (9), 1222–1233.
San-José, M.F., Caniego, F.J., 2013. Fractals and Multifractals in Pedodiversity and Biodiversity Analyses. In: Ibáñez, J.J., Bockheim, J.G. (Eds.), Pedodiversity. CRC Press, Boca Raton, p. 256 pp..
Santoro, A., Venturi, M., Agnoletti, M., 2020. Agricultural heritage systems and landscape perception among tourists. The case of Lamole, Chianti (Italy). *Sustainability* 12 (9), 3509. https://doi.org/10.3390/su12093509.
Savage, V.M., Gillooly, J.F., Woodruff, W.H., West, G.B., Allen, A.P., Enquist, B.J., Brown, J.H., 2004. The predominance of quarter-power scaling in biology. Funct. Ecol. 18, 257–282.
Schmidt, I., Dikau, R., 1999. Extracting geomorphometric attributes and objects from digital elevation models - semantics, methods, future needs. In: Dikau, R., Saurer, H. (Eds.), GIS for Earth Surface Systems - Analysis and Modelling of the Natural Environment E. S. Verlags b, Stuttgart, pp. 153–173.
Semhi, K., Abdalla, O.A.E., Khirbash, S.A., Khan, T., Asaidi, S., Farooq, S., 2009. Mobility of rare earth elements in the system soils–plants–groundwaters: a case study of an arid area (Oman). Arab. J. Geosci. 2, 143–150.
Semrau, J.D., DiSpirit, A.A., Gu, W., Yoon, S., 2018. Metals and methanotrophy. Appl. Environ. Microbiol. 84, e02289–e02317.
Serrano, E., Ruiz-Flano, P. (2007) Geodiversity. A theoretical and applied concept. *Geographica Helvetica* Jg. 62.
Song, et al., 2017. Effects of topography and vegetation on distribution of rare earth elements in calcareous soils. Acta Geochimica 36, 469–473.
Sørensen, R., Zinko, U., Seibert, J., 2005. On the calculation of the topographic wetness index: evaluation of different methods based on field observations. *Hydrol. Earth Syst. Sci. Discuss.* 2 (4), 1807–1834 ffhal-00301525f.
Stein, A., Gerstner, K., Kreft, H., 2014. Environmental heterogeneity as a universal driver of species richness across taxa, biomes and spatial scales. Ecol. Lett. 17, 866–880. https://doi.org/10.1111/ele.12277.
Syrbe, R.-U., Walz, U., 2012. Spatial indicators for the assessment of ecosystem services: Providing, benefiting and connecting areas and landscape metrics. Ecol. Indic. 21, 80–88.
Tibbett, M., Green, I., Rate, A., De Oliveira, V.H., Whitaker, J., 2021. The transfer of trace metals in the soil-plant-arthropod system. STOTEN 779, 146260.
Tukiainen, H., Toivanen, M., Maliniemi, T., 2022. Geodiversity and Biodiversity. In: From Kubalíková, L. (Ed.), Visages of Geodiversity and Geoheritage. Geological Society, London. Special Publications, 530.
Tuscany Region (2020) Uso e Copertura del Suolo della Regione Toscana. Decreto_n.18011_del_04-11-2020-Allegato-A, Regione Toscana, Direzione Urbanistica e Politiche Abitative/Settore Sistema Informativo Territoriale e Ambientale, Consorzio Lamma.
Tyler, G., 1996. Soil chemistry and plant distributions in rock habitats of southern Sweden. Nordic J. Bot. 16 (6), 609–635. https://doi.org/10.1111/j.1756-1051.1996.tb00279.x.
Tyler, G., 2004. Rare earth elements in soil and plant systems–A review. Plant Soil 267, 191–206.
Vai, G.B., 2001. Structure and stratigraphy: an overview. In: Vai, G.B., Martini, I.P. (Eds.), Anatomy of an Orogen: Northern Apennines and Adjacent Mediterranean Basins. Kluwer Academic Publ, Dordrecht, pp. 15–32.
Wang, X., Barrat, J.A., Bayon, G., Chauvaud, L., Feng, D., 2020. Lanthanum anomalies as fingerprints of methanotrophy. Geochem. Persp. Let. 14, 26–30.

Wang, L., Liu, H., 2006. An efficient method for identifying and filling surface depressions in digital elevation models for hydrologic analysis and modelling. Int. J. Geogr. Inf. Sci. 20 (2), 193–213.
Wang, L., Han, X., Ding, S., Liang, T., Zhang, Y., Xiao, J., Dong, L., Zhang, H., 2019. Combining multiple methods for provenance discrimination based on rare earth element geochemistry in lake sediment. Sci. Total Environ. 672, 264–274.
Wedepohl, K.H., 1995. The composition of the continental crust. Geochimica et Cosmochimica Acta 59, 1217–1232.
Wysocka, I., 2021. Determination of rare earth elements concentrations in natural waters – A review of ICP-MS measurement approaches. Talanta 221, 121636.
Wyttenbach, A., Furrer, V., Schleppi, P., Tobler, L., 1998. Rare earth elements in soil and in soil-grown plants. Plant Soil 199, 267–273.
Xie, et al., 2020. Mining and restoration monitoring of rare earth element (REE) exploitation by new remote sensing indicators in Southern Jiangxi, China. Remote Sens. 12 (21), 3558. https://doi.org/10.3390/rs12213558.
Youssef, F.B., Doumit, J.D., 2022. Morphometric analysis toward mapping relative tectonic activity of Lebanon. Paper in Appl. Geogr. 9 (2).
Yu, C., Huo, J., Li, C., Zhang, Y., 2022. Landslide displacement prediction based on a two-stage combined deep learning model under small sample condition. Remote Sens. 14 (15), 3732. https://doi.org/10.3390/rs14153732.
Yuan, et al., 2021. Effects of topography and soil properties on the distribution and fractionation of REEs in topsoil: A case study in Sichuan Basin, China. Sci. Total Environ. 15, 148404.
Zaharescu, et al., 2017. Ecosystem composition controls the fate of rare earth elements during incipient soil genesis. Sci. Rep. Nat. 7, 43208. https://doi.org/10.1038/srep43208.
Zarnetske, P.L., Read, Q.D., Record, S., Gaddis, K.D., Pau, S., Hobi, M.L., Malone, S.L., Costanza, J., Dahlin, K.M., Latimer, A.M., Wilson, A.M., Grady, J.M., Ollinger, S.V., Finley, A.O., 2019. Towards connecting biodiversity and geodiversity across scales with satellite remote sensing. Global Ecol. Biogeogr. 28, 548–556.
Zeng, F., Tian, H., Wang, Z., An, Y., Gao, F., Zhang, L., Li, F., Shan, L., 2003. Effect of rare earth element europium on amaranthin synthesis in Amarathus caudatus seedlings. Biol. Trace Elem. Res. 93, 271–282. https://doi.org/10.1385/bter:93:1-3:271.
Zhou, W., Han, G., Liu, M., Song, C., Li, X., 2020. Geochemical distribution characteristics of rare earth elements in different soil profiles in Mun River Basin, Northeast Thailand. Sustainability 12, 457. https://doi.org/10.3390/su12020457.